

**PERFORMANCE OF NANO-PARTICLE ASSISTED PHASE CHANGE
MATERIALS IN A SOLAR DESALINATION SYSTEM**

LIEW YUIN YUE


**A project report submitted in partial fulfilment of the
requirements for the award of Bachelor of Degree
(Honours) Mechanical Engineering**

**Lee Kong Chian Faculty of Engineering and Science
Universiti Tunku Abdul Rahman**

September 2022

DECLARATION

I hereby declare that this project report is based on my original work except for citations and quotations which have been duly acknowledged. I also declare that it has not been previously and concurrently submitted for any other degree or award at UTAR or other institutions.

Signature :  _____

Name : Liew Yui Yue _____


ID No. : 1806817 _____

Date : 3/10/2022 _____

APPROVAL FOR SUBMISSION

I certify that this project report entitled “**PERFORMANCE OF NANO-PARTICLE ASSISTED PHASE CHANGE MATERIALS IN A SOLAR DESALINATION SYSTEM**” was prepared by **LIEW YUIN YUE** has met the required standard for submission in partial fulfilment of the requirements for the award of Bachelor of Degree (Honours) Mechanical Engineering at Universiti Tunku Abdul Rahman.

Approved by,

Signature : 

Supervisor : Dr. Rubina Bahar
Date : 11/09/2022
Signature : _____
Co-Supervisor : _____
Date : _____

The copyright of this report belongs to the author under the terms of the copyright Act 1987 as qualified by Intellectual Property Policy of Universiti Tunku Abdul Rahman. Due acknowledgement shall always be made of the use of any material contained in, or derived from, this report.

© 2022, Liew Yuin Yue. All right reserved.

ACKNOWLEDGEMENTS

I would like to thank everyone who had contributed to the successful completion of this project. I would like to express my gratitude to my research supervisor, Dr.Rubina for her invaluable advice, guidance and his enormous patience throughout the development of the research.

In addition, I would also like to express my gratitude to my loving parents and friends who had helped and given me encouragement.

ABSTRACT

The goal of this study is to improve water production by using phase change material as a medium of thermal energy storage, which releases and absorbs energy while solar still exposed to sunlight. However, the weak thermal conductivity of PCM leads to low thermal energy storage capability. As a result, research into nanoparticles is critical. In these experiments, soft paraffin and paraffin wax were first tested to identify the performance of solar still. After that, nanoparticles were added to PCM with better performance to investigate the performance of PCM associated with nanoparticles. Paraffin wax possess better thermal conductivity than soft paraffin and provide a 3.11% higher in efficiency. Aluminium scrap as a replacement of alumina nano-powder did improve the solar still efficiency by 4.10% and give higher water productivity while SS with alumina nano powder was 3.42% higher efficiency. The result showed that for SS with NePCM containing alumina nano powder, SS with NePCM containing aluminium scrap and SS with pure PCM can produce 2.5g, 2.4g and 2.0g of water in RM 1 respectively. The payback period of the solar still without PCM, with pure PCM and NePCM (aluminium scarp w PCM and alumina nano powder with PCM) are 158, 149, 145 and 142 days, respectively. In short, the experiment shows that paraffin wax gives better thermal conductivity and nanoparticles enhanced the PCM thermal conductivity as it gives higher water productivity with less energy.

TABLE OF CONTENTS

DECLARATION		i
APPROVAL FOR SUBMISSION		ii
ACKNOWLEDGEMENTS		iv
ABSTRACT		v
TABLE OF CONTENTS		vi
LIST OF TABLES		viii
LIST OF FIGURES		x
LIST OF SYMBOLS / ABBREVIATIONS		xiii
LIST OF APPENDICES		xvi
CHAPTER		
1	INTRODUCTION	1
1.1	General Introduction	1
1.2	Importance of the Study	2
1.3	Problem Statement	3
1.4	Aim and Objectives	3
1.5	Scope and Limitation of the Study	3
1.6	Contribution of the Study	4
2	LITERATURE REVIEW	6
2.1	Introduction	6
2.2	Literature Review	6
2.2.1	Sensible Heat Storage	7
2.2.2	Chemical Reaction Heat Storage	8
2.2.3	Latent Heat Storage	9
2.2.4	Parameter of TES System	10
2.3	Phase Change Material Classifications	11
2.3.1	Selection criteria of Phase Change Material	13
2.4	Nanoparticles with PCM	14
2.4.1	Concentration of nanoparticles	15

	2.4.2	Sizes of nanoparticles	15
	2.5	Solar still	16
	2.5.1	Type of solar still	17
	2.6	Factors affecting solar still's water productivity	19
	2.6.1	Climatic parameters	19
	2.6.2	Design Parameter	20
	2.6.3	Operational Parameter	24
	2.7	Summary	25
3		METHODOLOGY AND WORK PLAN	26
	3.1	Introduction	26
	3.2	Mathematical Model of Basin Type Solar Still	27
	3.3	PCM Selection	30
	3.3.1	Data and Preparation of Organic PCMs	32
	3.4	Nanoparticles Selection	34
	3.4.1	Data and Preparation of nanoparticles	34
	3.5	Design of PCM storage	35
	3.6	Experiment Planning	36
4		RESULTS AND DISCUSSION	38
	4.1	Introduction	38
	4.2	Experiment	38
	4.3	Temperature	40
	4.3.1	Experiment on PCM effects	41
	4.3.2	Experiment on PCM enhanced by nanoparticle	43
	4.4	Water productivity and Solar Still Efficiency	48
	4.5	Water Conductivity	52
	4.6	Cost Analysis	52
	4.7	Challenges	54
5		CONCLUSIONS AND RECOMMENDATIONS	56
	5.1	Conclusions	56
	5.2	Recommendations for future work	57
		REFERENCES	59
		APPENDICES	66

LIST OF TABLES

Table 2.1:	Typical parameters of thermal energy storage system (Dinesh, 2008)	11
Table 2.2:	Thermal conductivity after addition of nanoparticle at different concentration (Nourani, et al., 2016)	15
Table 2.3:	Melting temperature and laten heat of PCM at different concentration (Nourani, et al., 2016)	15
Table 2.4:	Comparison between Passive and Active solar still	18
Table 2.5:	Still's output by different insulation thickness (Elango and Kalidasa Murugave, 2014)	24
Table 3.1:	Comparison on organic and inorganic PCMs	31
Table 3.2:	Benefits and Drawbacks of 3 types of PCMs	32
Table 3.3:	Difference between paraffin and fatty acids on environmental effect	33
Table 3.4:	Thermal cycle test for palm and paraffin waxes (T. Trisnadewi et al, 2021)	33
Table 3.5:	Cost comparison of PCMs	34
Table 3.6:	Comparison on nanoparticle price and thermal conductivity	35
Table 4.1:	SS efficiency of model A, B, C	48
Table 4.2:	SS efficiency of model B and D	50
Table 4.3:	SS efficiency of model E and D	51
Table 4.4:	TDS values of water before and after experiment	52
Table 4.5:	Cost analysis on PCM	52
Table 4.6:	Cost analysis on nanoparticle	53
Table B.1:	Properties of Organic PCMs (Paraffin)	71
Table B.2:	Properties of Organic PCMs (non-Paraffin)	72
Table B.3:	Specification of solar stills	73

Table B.4:	PCM specifications	73
Table B.5:	Aluminium scarp and alumina nanopowder specifications	74
Table B.6:	Raw material cost for one model	74
Table B.7:	Payback period of solar still without PCM, with pure paraffin wax, with NepCM (Al scrap and Alumina nano powder)	75

LIST OF FIGURES

Figure 2.1:	Classification of TES (Zhi Li, et al, 2021)	6
Figure 2.2:	Principle of thermochemical storage (e-hub, n.d.)	8
Figure 2.3:	Principle of latent heat storage (Reddy, et al, 2018)	9
Figure 2.4:	PCM Classification (Jerol, 2018)	12
Figure 2.5:	Desirable properties of PCM	14
Figure 2.6:	Concept of solar still (Derek, et al., 2020)	17
Figure 2.7:	Classification of Solar Still (Abdel, et al., 2018)	17
Figure 2.8:	Factors influencing solar still output	19
Figure 2.9:	Still's productivity varies with tilt angle in different seasons (Suresh, et al., 2017)	21
Figure 2.10:	Effect of water salinity percentage on solar still productivity (Akash, et al., 2000)	25
Figure 3.1:	Flow chart of works	26
Figure 3.2:	Heat transfer inside SS (Abhay, et al., 2017)	27
Figure 3.3:	Design of single slope solar still in this study	36
Figure 3.4:	Procedure of preparing PCM with nanoparticle. (Al-Yasiri and Szabó, 2021)	37
Figure 4.1:	Condition of PCMs before and after experiments	38
Figure 4.2:	Condition of NePCMs before and after experiments	39
Figure 4.3:	Experiment setup	39
Figure 4.4:	Prototype of Solar Still with tilt angle at 19°	40
Figure 4.5:	Graph of SS without PCM (model A)	41
Figure 4.6:	Graph of SS with Paraffin wax (model B)	41
Figure 4.7:	Graph of SS with Soft paraffin (model C)	42
Figure 4.8:	Graph of SS with Paraffin wax (model B)	44

Figure 4.9:	Graph of SS with Paraffin wax with Al scrap (model D)	44
Figure 4.10:	Graph of SS with Paraffin wax with Al ₂ O ₃ nanopowder (model E)	46
Figure 4.11:	Graph of SS with Paraffin wax with Al scrap (model D)	46
Figure 4.12:	Daily water yield and water productivity of Model A, B, C	48
Figure 4.13:	Water productivity and SS efficiency of Model A, B, C	48
Figure 4.14:	Daily water yield and water productivity of Model B and D	49
Figure 4.15:	Water productivity and SS efficiency of Model B and D	49
Figure 4.16:	Daily water yield and water productivity of Model E and D	50
Figure 4.17:	Water productivity and SS efficiency of Model E and D	50
Figure 4.18:	TDS value of water before and after experiment	52
Figure A.1:	TDS water chart (Jeff Wahl, 2021)	66
Figure A.2:	Convective heat transfer of 3 model in 1 st experiment (calculate based on experiment data).	66
Figure A.3:	Evaporative heat transfer of 3 model in 1 st experiment (calculate based on experiment data).	67
Figure A.4:	Radiative heat transfer of 3 model in 1 st experiment (calculate based on experiment data).	67
Figure A.5:	Convective heat transfer of model B and D in 2 nd experiment (calculate based on experiment data).	68
Figure A.6:	Evaporative heat transfer of model B and D in 2 nd experiment (calculate based on experiment data).	68
Figure A.7:	Radiative heat transfer of model B and D in 2 nd experiment (calculate based on experiment data).	69
Figure A.8:	Convective heat transfer of model E and D in 3 rd experiment (calculate based on experiment data).	69
Figure A.9:	Evaporative heat transfer of model E and D in 3 rd experiment (calculate based on experiment data).	70

Figure A.10: Radiative heat transfer of model E and D in 3rd experiment
(calculate based on experiment data).

LIST OF SYMBOLS / ABBREVIATIONS

c_p	specific heat capacity, J/(kg·K)
Q	heat transferred, J
m	material's mass, kg
V	volume of material, m ³
Δh_m	latent heat of fusion per unit mass, kJ/kg
Δh_r	endothermic heat of reaction, kJ/kg
ΔT	temperature difference at initial and final stage, °C
T_i	temperature at initial stage, °C
T_f	temperature at final stage, °C
T_m	temperature at melting stage, °C
C_p	specific heat capacity of material, J/kg·K
C_{sp}	average specific heat between initial and melting temperature, kJ/kg·K
C_{lp}	average specific heat between initial and melting temperature, kJ/kg·K
T_w	water temperature, °C
T_g	cover temperature, °C
q_{cwg}	convective heat transfer among water cover surface, W/m ² °C
q_{ewg}	evaporative heat transfer among water cover surface, W/m ² °C
q_{rwg}	radiative heat transfer among water cover surface, W/m ² °C
p_w	water surface pressure, N/m ²
p_g	cover inner surface pressure, N/m ²
A_w	evaporation area, m ²
$h_{fg, sw}$	SW latent heat of vaporization (kJ/kg)
$h_{fg, w}$	water latent heat of vaporization (kJ/kg)
E	energy used, kJ
P	solar power, W
m_{yield}	mass yield, kg
K_{npcm}	thermal conductivity of NePCM, W/mK
K_{pcm}	thermal conductivity of PCM, W/mK
K_{np}	thermal conductivity of nanoparticle, W/mK
$C_{p_{pcm}}$	specific heat of PCM, J/kg K

$C_{p_{npcm}}$	specific heat of NePCM, J/kg K
$C_{p_{np}}$	specific heat of nanoparticle, J/kg K
T	temperature of NePCM, K
T_{ref}	Reference temperature, K
T_{solids}	temperature of NePCM at solid state, K
$T_{liquids}$	temperature of NePCM at liquid state, K
d_{np}	diameter of nanoparticle, m
L_{npcm}	latent heat of NePCM, J/kg
L_{pcm}	latent heat of PCM, J/kg
n_{pb}	payback period
$S_{p,w}$	water price, RM
i_r	interest rate
P_c	capital cost
a_r	fraction melted/reacted
S	water salinity

Greeks

ρC_p	energy density
ρ	density, kg/m ³
ε_{eff}	effective emissivity of water to cover surface
ε_w	emissivity of water
ε_c	emissivity of cover
σ	Stefan Boltzman' s constant
ϕ	volumetric fraction of nanoparticle
ζ	Brownian motion correction factor

Abbreviations/ Subscripts

PCM	Phase Change Material
NePCM	Nanoparticle enhanced Phase Change Material
TES	Thermal Energy Storage
SDG	Sustainable Development Goal
UiTM	Universiti Teknologi MARA
LHS	Latent Heat Storage

SSSS	Single Slope Solar Still
DSSS	Double Slope Solar Still
SW	Saline Water

LIST OF APPENDICES

Appendix A: Figures	66
Appendix B: Tables	71

CHAPTER 1

INTRODUCTION

1.1 General Introduction

Water shortage affects about two-thirds of human existence, and many of these developing countries also lack reliable electricity. Human rights are intrinsically tied to water shortages and guaranteeing adequate access to safe drinking water is a global development concern. However, many nations and large cities throughout the world encountered worsening water shortages in the twenty-first century as a result of population expansion, overconsumption, increased pollution, and climate changes caused by global warming.

Water is essential for the survival of all living things as water accounts for 60% of body physical weight. Without water, there would be no life on earth. Water is required by bodies to assist control body temperature and sustain other physical processes. It is consisted in all cells, organs, and tissues. There are two sorts of water scarcity: economic and physical or absolute scarcity. Economic water shortage is caused by lack of water infrastructure, and it have affected 1.6 billion peoples. Physical or absolute water shortage is when the demand for water supplies exceeds the availability. There are 1.2 billion peoples live in locations where physical resources are scarce.

There are only 2.6 % of all water on the planet is pure, whereas 97.4 % is salt water. 780 billion of people can't get access to clean water. Rural area in Africa, woman travels 6 km each day to collect 18 kg of water. Contaminated water and poor sanitation have causing almost 800 kids die every day as a result of diarrhoea. In water-stressed nations, population of 733 million out of 2.3 billion people living in high and severely water-stressed countries. Over half of the world's population spends at least 1 month each year in potentially water-scarce areas, and this figure is predicted to climb to 4.8–5.7 billion by 2050. Around 73% of population living in Asia is affected. (69% by 2050).

To solve these issues, a lot of study has gone into finding techniques to desalinate saltwater or brackish water with several methods such as, filtration, sedimentation, distillation, sand filters, flocculation and via ultraviolet light. All these technologies are capable of purifying polluted water by killing

germs or removing salts from it, resulting in access to fresh water for humans. However, some of these systems had a high running cost, hence solar desalination became the most common approach for distilling water from salt water due to its affordable installation and maintenance costs and independent water production that just required solar energy to function.

In conventional solar distillation system, the performance is relatively poor and do not able to produce sufficient volume of fresh water as it solely dependent on sunlight to generate energy causing the system could not work on nigh time, cloudy day and rainy day. Due to this reason, a lot of research have done to figure out the solution. It is found that phase change material (PCM) can act as thermal energy storage (TES) medium by adding it into the solar still to improve the thermal efficiency of the system. Although the phase change material can help to store energy during the daytime and enable the solar still operate for whole day, but the improvement of the system productivity still little for producing sufficient volume of clean drinking water due to the phase change material have a quite low thermal conductivity.

In this study, it is an investigation on which are the most suitable phase change material and nanoparticle that can overcome the thermal conductivity problem of phase change material and water production to settle the low water productivity of solar desalination system while keeping it low cost.

1.2 Importance of the Study

The study's findings are expected to improve and optimise water production from solar still while using phase change material (PCM) as a thermal energy storage. By adding phase change material into the system and assisting it with conductive nanoparticles, the performance of solar distillation may be enhanced. As a result, a clearer picture of PCM's function in thermal energy storage will develop in this work.

The goal of this research is to increase the efficiency and performance of solar desalination systems while lowering construction costs in order to alleviate water shortages using a low-cost, low-maintenance technology.

1.3 Problem Statement

Since traditional solar distillation systems are ineffective at purifying water, the volume of distilled and fresh water available is still insufficient to address the rural water problems. As a result, a variety of phase change materials and nanoparticles have been utilised in various studies to boost freshwater production.

Traditional solar still systems rely on direct solar radiation to create energy for freshwater production by heating saline water until evaporation occurs; however, this limits the system's effectiveness because it can only operate during daylight hours. As a consequence, phase change materials are used, however the majority of them have limited heat conductivity.

As the thermal energy storage capability of phase change material is low due to weak thermal conductivity, the system's thermal conductivity can be improved using nanoparticles. The target of this study is to compare and determine the most suitable combination of phase change material and nanoparticles for solar desalination systems with the highest efficiency.

1.4 Aim and Objectives

The purpose of this research is to improve the water production by using phase change material as medium of thermal energy storage while improving its thermal conductivity with nanoparticles to optimize the solar desalination system's efficiency. Hence, below are the study's objectives:

1. To identify the suitable phase change material (PCM) for increased production from a solar still
2. To determine the optimum conductive nanoparticle to be associated with the PCM.
3. To evaluate the performance and economic viability of the solar still.

1.5 Scope and Limitation of the Study

The scope of this research is finding the data and information of phase change material and nanoparticles. After data is collected, suitable material for phase change material and nanoparticle is selected. Experiment will be conducted to

verify the performance of selected phase change material and nanoparticle in solar desalination.

The limitation in this study is the cost of material. As the cost of material is always taken into consideration, there is a limitation on material's selection. In particular, nanoparticle have relatively higher thermal conductivity are also pricier. Besides, in Malaysia, petroleum is the primary source of electricity generation and is rich in mineral resource hence is self-sufficient in energy production. In this case, solar energy is still not a trend in Malaysia hence phase change material can be found in Malaysia is still little.

1.6 Contribution of the Study

There are four types of water treatment in Malaysia: reverse osmosis, filtration, UV, and distillation. The distillation process is superior to any other method of water treatment since it removes all contaminants from the water. The water stress level was also estimated to be more serious over time in worldwide.

In this research, the nanoparticle was used to assist the PCM to improve its thermal conductivity to enhance the solar distillation performance. To prove the theory, nano powder will add to the PCM to enhance its thermal conductivity in order to increase SS efficiency. Moreover, not only using nano powder to conduct the experiment but aluminium scrap was also used as a replacement of nano powder to indicate whether it could give the similar efficiency of alumina nano powder in enhancing the PCM thermal conductivity. A comparison on aluminium scrap and nano powder will be done. The cost of nano powder is expensive, if aluminium scrap could give similar efficiency, it will be lower the cost of the SS system.

This study could bring clean water to the society and worldwide, also moving towards the SDG by providing clean water and sanitation, use of affordable and clean energy. Due to the climate change, solar energy will be more efficiency in the future, and it is worth to investigate. This study could help people in high water stress regions such as Africa and India to obtain clean water and better sanitation with cost consideration. Last but not least, this study could also provide future researchers a data and analysis on the improvements that can be done to SS and the alternative method that might can

be used to enhance the PCM and may explore on other method or type of nanoparticle to increase the efficiency of solar desalination.

CHAPTER 2

LITERATURE REVIEW

2.1 Introduction

In this chapter, several references of related journals, articles, report, theoretical and experimental studies, and research papers is taken to conduct the study on performance of nanoparticles assisted phase change materials in solar desalination.

2.2 Literature Review

Energy storage technologies are extremely practical because their potential to change the incompatibility between energy transmission and energy demand that applicable for alternative energy sources like solar and wind. Thermal energy storage is the preferred method for a wide range of applications, including solar water heaters and air conditioners. In TES systems, three types of energy storage technologies are used: sensitive heat, latent heat, and thermochemical approaches. (Hadi Bashirpour-Bonab, 2021)

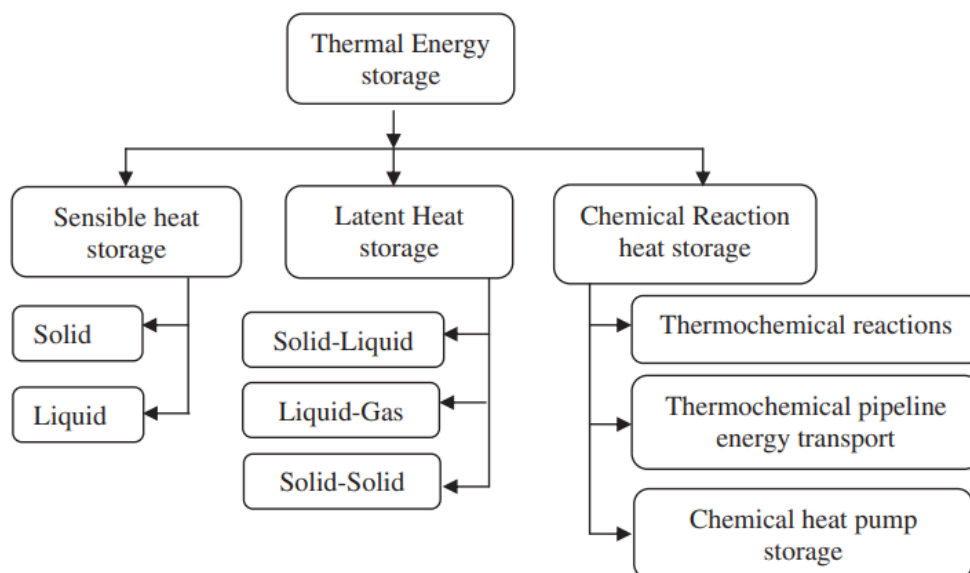


Figure 2.1: Classification of TES (Zhi Li, et al, 2021)

As solar energy is irregular and inconsistent causing the reliability of its usage in thermal application is still relatively low as demand over supply. In

an efficient TES system, energy should store whenever it is available to ensure it can be used for hours without sunlight. The thermal energy storage system will alleviate the energy demand-supply mismatch, consequently enhancing the system's performance and lowering the costs associated with energy loss.

In particular, storage could increase the reliability of power plant by balancing load. As the efficiency of energy system enhance, result in reduction in cost and energy consumption is lower. Some renewable energy sources can only deliver power on a sporadic basis.

2.2.1 Sensible Heat Storage

In sensible heat storage approach, energy is stored based on the medium's specific heat capacity by varying temperature which mean a liquid or a solid (such as water, molten salts, sand, or rocks) is either undergo heating or cooling process to stored or retrieve energy while no phase change during the charging or discharging process. In short, heat energy is stored, and the material is heat up when heat energy is dissipated, the material is cool down.

A lot of different material or substances have been utilised in this system as medium of thermal energy storage. Example of liquids are water, heat transfer oils (e.g., mineral oil and engine oil) and molten salts (e.g., carbonate salt), whereas concrete, limestone, cast iron and brick are examples of solids. For solid substances which is usually porous, energy is stored or removed when gas or liquid pass through the holes or gaps.

The temperature variation and storage substance's specific heat capacity define the storage substance's sensible heat change. The sensible heat storage is determined by Equation 2.1 below.

$$Q = mC_p\Delta T = V\rho C_p\Delta T \quad (2.1)$$

where,

Q = Heat transferred, J

m = material's mass, kg

C_p = specific heat capacity of material, J/kg•K

ΔT = T_f – T_i, temperature difference at initial and final stage, °C

V = volume of material, m³

ρ = density of material, kg/m³

ρC_p = energy density

2.2.2 Chemical Reaction Heat Storage

In thermochemical storage system, energy is store and extract by breaking and rebuilding the molecule linkage it is also known as reversible chemical process. In this storage system, there are charging, storing, and discharging process. The principle of thermochemical storage is illustrated in Figure 2.2.

First, in endothermic reaction, heat is received from energy source separate the substance A into reactants B and C: Reactants B and C is stored at room temperature to ensure no thermal losses after the charging step. Energy is released (used as energy source) and reactant A is formed during the exothermic process when substance B and C are mixed.

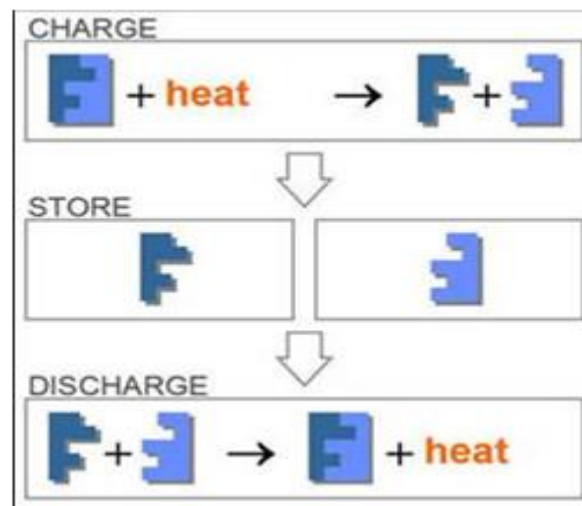
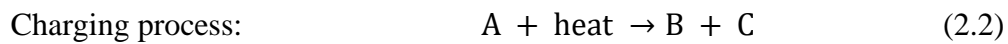


Figure 2.2: Principle of thermochemical storage (e-hub, n.d.)

In this storage system, the storage capacity is dependent on the amount of substances, rate of conversion and heat reaction. Chemical reaction heat transferred can be expressed in Equation 2.4 below.

$$Q = a_r m \Delta h_r \quad (2.4)$$

where

Q = heat transferred, J

m = material's mass, kg

a_r = fraction reacted

Δh_r = endothermic heat of reaction

2.2.3 Latent Heat Storage

Latent heat storage is based on the principle of latent heat of fusion of storage material when it undergoes phase change. Heat energy is absorbed when solid is melting into liquid and energy is stored during the phase change which also known as latent heat. Due to the rise in temperature, the molecular bond of PCM break apart causing transition from 1 phase to another, temperature at the phase transition is almost constant. When the substances are crystalline from liquid to solid, heat is released.

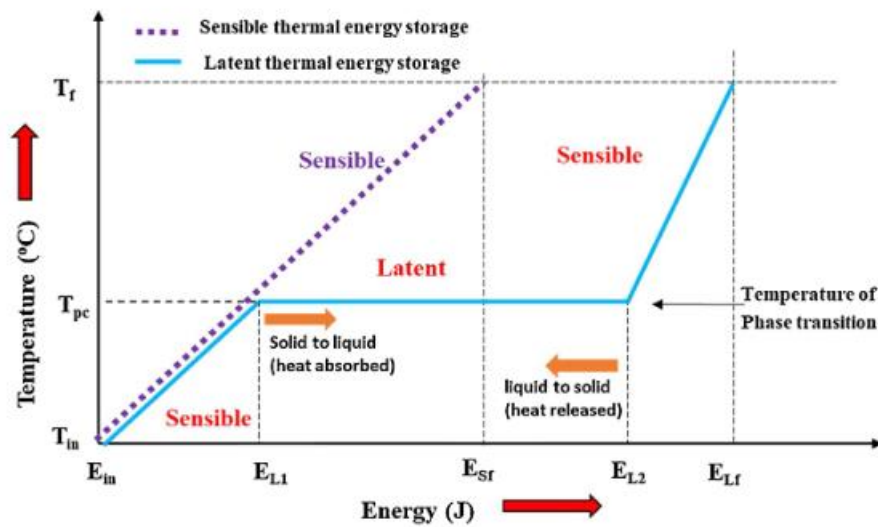


Figure 2.3: Principle of latent heat storage (Reddy, et al, 2018)

Transition from liquid to gas is not suitable for thermal energy storage as require high pressure and relatively big volume to store heat in gaseous state. In addition, solid to solid (e.g., polymer and polyalcohol) transition have lower latent heat, although it has smaller volume change and better design freedom, but the amount of energy stored is lesser. The process of latent heat system is exclusively physical and normally for application with steady temperature. The heat energy of the latent heat storage system is given as Equation 2.5 below:

$$Q = m[C_{sp}(t_m - t_i) + a_m \Delta h_m + C_{lp}(t_f - t_m)] \quad (2.5)$$

where

Q = heat transferred, J

m = material's mass, kg

a_r = fraction melted

Δh_m = latent heat of fusion per unit mass, kJ/kg

T_i = temperature at initial stage, °C

T_f = temperature at final stage, °C

T_m = temperature at melting stage, °C

C_{sp} = average specific heat between initial and melting temperature, kJ/kg•K

C_{lp} = average specific heat between melting and final temperature, kJ/kg•K

2.2.4 Parameter of TES System

There are some parameters to define the performance of the thermal energy storage:

1. Power capacity define when discharging, the largest power that the storage system can provide;
2. Power density define the proportion of system capacity to the power capacity;
3. Energy storage capacity refer to how much energy is stored throughout the charging process;
4. Energy density is also known as volumetric heat capacity;
5. Storage periods define how long the energy will be kept;
6. Response time refers to the rate at which energy is absorbed and released speed in a system;
7. Cycle life represent the total number of cycle of charge-discharge;
8. Discharge rate is the rate of stored energy released;
9. Self-discharge is the loss of energy over a period of time while the device is not in use or idle mode;
10. Cycle efficiency η is E_{out}/E_{in} ; the losses in idle mode is not taken into consideration;
11. Costs refer to storage capacity (RM/kWh) of the system, and relate to the initial, running and maintenance cost of the storage apparatus.
12. Cost per output is calculated by dividing the cost of useable energy by the storage efficiency;

Table 2.1: Typical parameters of thermal energy storage system (Dinesh, 2008)

TES System	Capacity (kWh/t)	Power (MW)	Efficiency (%)	Storage period (h, d, m)
Sensible (hot water)	10-50	0.001-10	50-90	d/m
PCM	50-150	0.001-1	75-90	h/m
Chemical reactions	120-250	0.01-1	75-100	h/d

The latent heat storage have larger storage capacity and adiabatic retention function hence it's had more procedure. Compare with sensible heat storage approach, phase change material in latent thermal energy storage system can store 5 to 14 times of same volume. Moreover, most PCMs have a low favourable thermal conductivity, which considerably minimises the energy charge/discharge measure and assures that system reaction time satisfies extremely lengthy conditions.

The latent heat is much higher than the sensible heat for a given medium, and it is also suitable for most applications because of its high energy storage density requiring only small temperature variations.

2.3 Phase Change Material Classifications

Phase change materials (PCM) are storage material in the latent heat storage system. PCM may be used to regulate temperature in variety of system as it melts and freeze at certain. Heat energy can be better absorbed by material when the substances is melting. This indicates that storing energy in PCM require noticeably less quantity of material compared to material required in sensible heat storage where the process does not involve phase transition.

Different materials will have different chemical properties and characteristics, for example, melting point, freezing point, and specific heat capacity. The PCM is divided into 3 groups which is organic, inorganic and eutectic as shown in Figure 2.4 below.

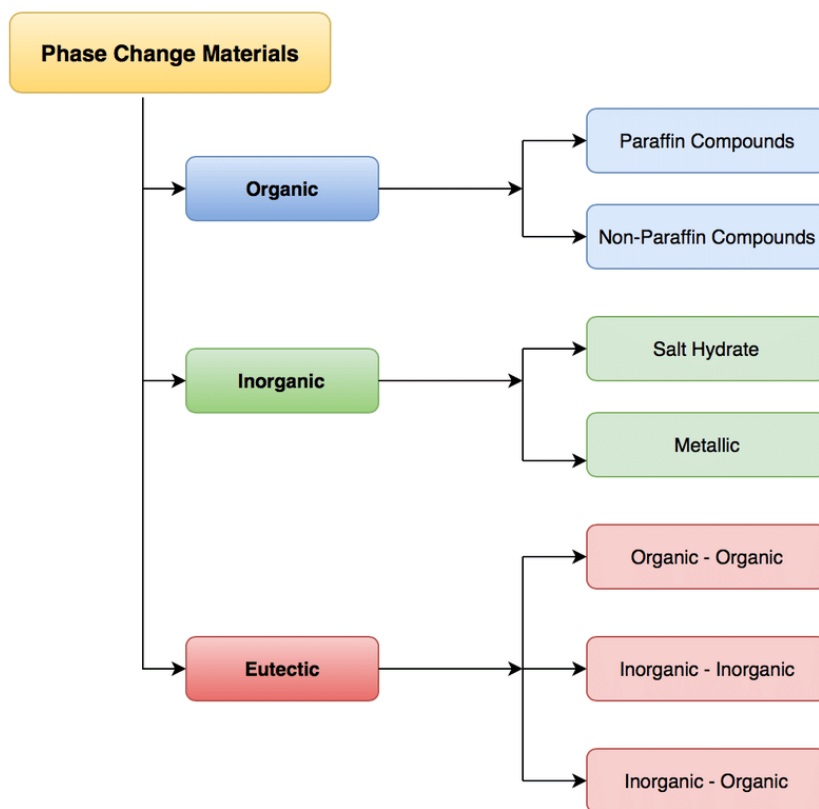


Figure 2.4: PCM Classification (Jerol, 2018)

Organic PCM can be categorized into paraffin compounds and non-paraffin compounds. Organic PCM typically consists of carbon atom. PCM classified in the group of paraffin are normally with a chemical formula of C_nH_{2n+2} , whereas functional group like fatty acids (R-COOH), alcohols (-OH), boxylic acids (CO₂H), and esters (CO₂R) are found in non-paraffin compound. For paraffin compound, the greater number of carbon atom, the higher the melting temperature and latent heat. The temperature range of organic PCMs is considerable wide, it can maintain it stability up to 300°C. There are several benefits of using organic PCM as it is chemically inert, recyclable, do not undergo phase separation, stable for repeated cycles and can used with most containers. Though there are many advantages but there are also some downsides on organic PCM such as thermal conductivity is low, not compatible with plastic container when it is in high temperature and moderately flammable.

For inorganic PCMs, there are 2 main types which are salt hydrate and metallic. Salt hydrate is an alloy of the combination of inorganic salt and n kilomole of water. Through dehydration and hydration process, a crystalline

solid is created. After melting, a salt hydrate with fewer moles of water or a salt hydrate with more moles of water is formed. For the group of metallic, it also consists of metal and alloy with low melting temperature. In this category, the material has high thermal conductivity, low vapor pressure and low specific heat. Thus, inorganic PCM is more suitable for application require higher temperature up to 1500°C. Advantages of inorganic PCM are it is non-flammable, cheap, high thermal conductivity, and sharp phase transition. The drawback of it is phase segregation during transition, material durability, corrosive to metal and chemical stability decrease after few cycles.

Eutectic materials can be mixture of organic and organic compounds, inorganic and organic compounds and inorganic and inorganic compounds, can be 2 or more materials in a combination. Eutectic PCM usually have good thermal conductivity and density, it will melt and freeze uniformly without any dispersion. The principle of it is when various compounds melt at the same time, or when it is freeze to an intimate mixture of crystals, chances of compound segregation is reduced. This is the optimum state of PCM, although it is less dispersed as the cost of producing an eutectic PCM is much higher.

2.3.1 Selection criteria of Phase Change Material

Also, there are several criteria on selecting the PCM based on the application. For most application, the temperature range of PCM is crucial during the design. It is important to analyze thermo-physical properties, stability, and reliability before selecting PCM.

Thermo-physical properties that needed taken into consideration are, density, latent heat of fusion, thermal conductivity, melting temperature and specific heat capacity of the materials. For instances, in latent heat storage system, it is vital to have a material with high latent heat so more heat energy can be stored while low melting point and good thermal conductivity is preferred to supply higher efficiency. However, it is also necessary to considered it from other aspect.

There are several aspects need to be considered on selecting PCM for solar energy applications which is thermal, physical, kinetic, chemical, and economic properties. A desirable PCM from the various aspects is listed in the Figure 2.5 below.

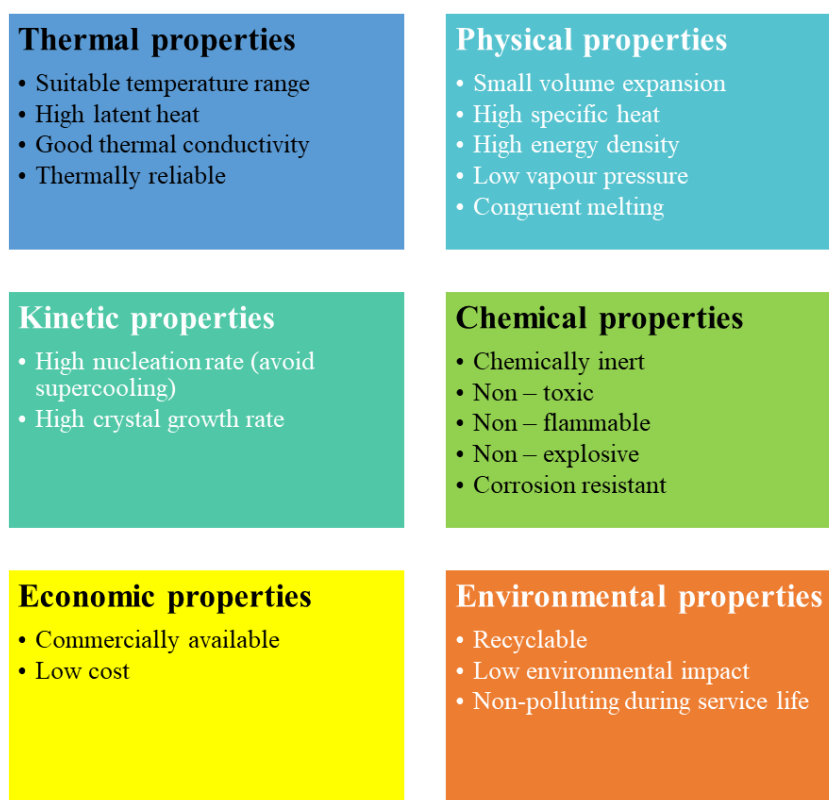


Figure 2.5: Desirable properties of PCM

2.4 Nanoparticles with PCM

To overcome the low thermal conductivity of PCM problem, various solutions are developed through changes in PCM container structure or adding additives into PCM, for example sinking the fin, installing heat pipes, embedding metal foams, and spreading highly conductive nanoparticles. With the aid of nanoparticle, shortcoming of PCMs can be overcome. As reported, PCMs assisted with nanoparticles can improve energy performance and temperature control hence it is used for speed up unstable process and enhance performance.

There are 2 common types of methods, encapsulation and adding nanomaterial into PCM. For adding nanomaterial approach, the nanomaterial are usually metals, metal oxides and carbon-based substances, and it will incorporate with PCM. Encapsulation can also give similar benefits and additional benefits of encapsulation is it give protection to PCM from environment outside. Besides that, study of encapsulation in current level is still stagnant on micro and macro-encapsulation, research in nano-encapsulation is still scarce it might be due to the cost of production.

2.4.1 Concentration of nanoparticles

Nourani, et al. (2016) state that, the thermal conductivity of paraffin increases with the increase of nanoparticle concentration as shown in Table 2.2 below. In the research, it proved that by dispersing 2.5, 5.0, 7.5, and 10.0% of alumina nanoparticle, the time required to heat the paraffin was shrunked by 2, 18, 21 and 27% respectively, also, this result in a increase in melting rate by 9, 20, 24, and 27% respectively as compared to pure paraffin. Revealing that the thermal conductivity of PCM improved significant as a function of nanoparticle weightage and demonstrating that the influence of nanoparticle dispersion in PCM is significant in the range of melting temperature. According to Arasu, et al. (2011), performance of heat transfer improved as the rate of melting of paraffin wax increase by 4.8% with the dispersion of 1% of Al_2O_3 nanoparticle. Also, melting time were shortened by 27% with 10% increase in mass concentration but the heat capacity of the paraffin wax also decreased.

Table 2.2: Thermal conductivity after addition of nanoparticle at different concentration (Nourani, et al., 2016)

Average values of effective thermal conductivity for composites and pure paraffin in solid and liquid states.

Sample concentration (wt.%nano- Al_2O_3)	Average effective thermal conductivity (W/m °C) (Solid state)	Average effective thermal conductivity (W/m °C) (Liquid state)
0 (paraffin)	0.197	0.148
2.5	0.227	0.152
5.0	0.236	0.156
7.5	0.245	0.162
10.0	0.259	0.167

Table 2.3: Melting temperature and laten heat of PCM at different concentration (Nourani, et al., 2016)

Melting temperatures and latent heats of pure paraffin and nanocomposites at different nanoparticle concentrations (mean value \pm SD).

Sample concentration (wt.%nano- Al_2O_3)	Melting temperature (°C)	ΔT_m ($T_{m_NCPM} - T_{m_paraffin}$) (°C)	Latent heat (kJ/kg)	ΔL ($L_{NCPM} - L_{paraffin}$) (kJ/kg)
0 (Paraffin)	60.00 \pm 0.71	0	204.28 \pm 4.64	0
2.5	61.20 \pm 0.99	1.20	200.16 \pm 4.32	-4.12
5.0	61.50 \pm 0.71	1.50	198.87 \pm 6.53	-5.41
7.5	61.35 \pm 2.05	1.35	189.42 \pm 2.01	-14.86
10.0	61.65 \pm 0.64	1.65	182.28 \pm 6.05	-22

2.4.2 Sizes of nanoparticles

Based on Deepti and Amos (n.d.) experiment research, it was revealed that the smaller the nanoparticle size, the higher the solar still productivity. From the research, it showed that, 10nm of nanoparticle can improved solar still productivity by 26.46% while 50nm nanoparticle only able to improve water

production by 1.46%. This is due to smaller particle allow faster rate of heat transfer.

2.5 Solar still

A solar still which also known as solar water distiller. It is a type of green energy to purify water. It is originally built for army and naval flyers forced down in the sea, this gadget turns saline water or polluted water into drinking water by evaporation and condensation caused by the sun's rays. Solar stills may thus provide fresh drinkable water and for cooking even in regions that have no other sources of electricity, while being pollution free. There are 2 working principle of solar still which involve evaporation and condensation.

Concept of a solar still is simple to understand. The salt water was poured to a basin to a particular depth. To better collect sun's short-wave energy, the basin's internal surfaces are blackened by coating such as paint. A slanted clear cover covering the basin and optimizes solar energy transfer. Saltwater starts to be heated as sunlight is absorbed and the basin cover; the temperature and vapour pressure of water increase when the duration of solar still exposed to sunlight increase. The water turns into steam and rise to the glass ceiling.

As shown in Figure 2.6 below, water evaporate and hit the ceiling, water vapour condenses underneath the slanted transparent cover then water will flow to the downhill through the transparent cover to the water collection channel. The accumulated water is a distilled solution that is free of contaminants and safe to consume. It can generate high quality water without other energy sources such as fossil fuel. Water vaporisation only occur when water molecules existing at water-air interface, there will also have heat losses during the energy transmit to the volume of water underneath the water surface for the vapor being generated. Consequently, the performance and production rate of the solar still is not favourable.

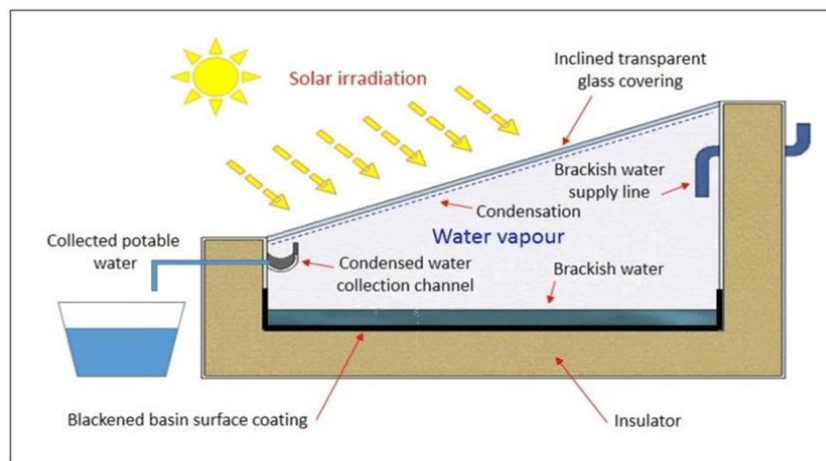


Figure 2.6: Concept of solar still (Derek, et al., 2020)

2.5.1 Type of solar still

As shown in Figure 2.7 below, solar still can be classified into 2 type which are active and passive.

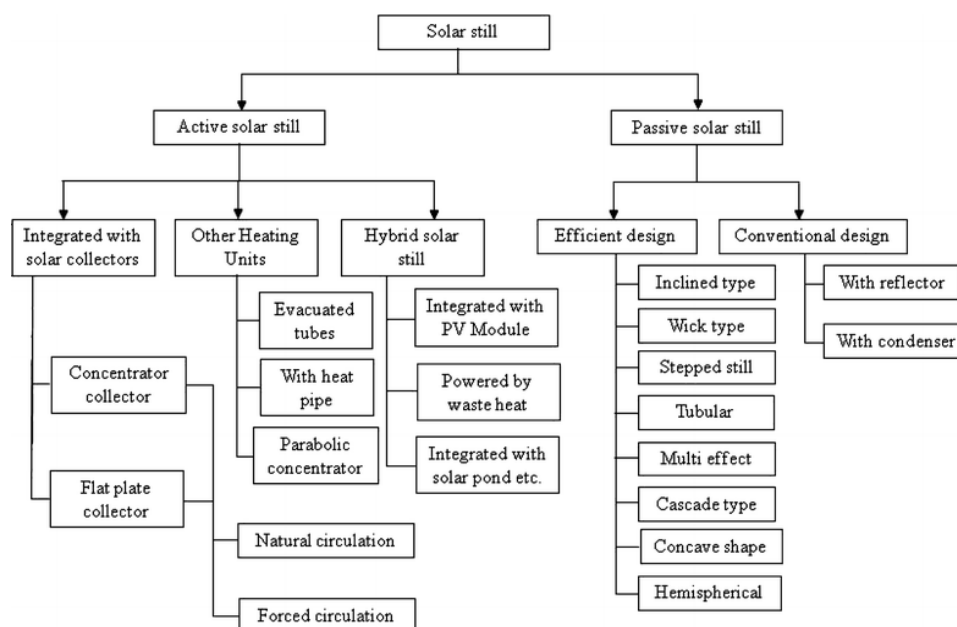


Figure 2.7: Classification of Solar Still (Abdel, et al., 2018)

2.5.1.1 Active Solar Still

Mechanical or electronic systems are utilized in active solar still as auxiliary energy to harvest and distribute solar energy. The most common device capturing solar energy is solar panels. Solar panels are made up by linking a series of solar cells that harness the sunlight to create and provide energy. Various devices such as sensors, controllers, pumps are used in active solar still

to optimise energy collecting and delivery automatically. Solar trackers placed in active photovoltaic panels may have built-in detectors and actuators to assist in tracking the sun's path across the sky. The drawback of active solar still is that they need to be maintained. They may also fail if auxiliary power supplies malfunction.

2.5.1.2 Passive Solar Still

Mechanical or electronic systems are not needed in passive solar still to collect and distribute solar irradiance. Hence, walls, floors, and windows, have been constructed or designed to harvest solar energy in a building, store it, then distribute it. This system is designed to redirect solar heat when demanded and alter air flow for circulation or heating water with the minimum reliance on external sources of energy. For instances, solariums, sunrooms, and greenhouses are all passive solar designs. There're also passive devices that involve traditional energy sources to regulate dampers, shutters, night insulation, and other appliances that aids in the gathering, storing, and utilization of solar irradiance. Previously, more complicated passive solar energy was designed such as solar forge and solar furnace however, these were not adopted due to its cost. Currently, uses of passive solar energy in water, space, and heating have been discovered to be cost-effective.

Table 2.4: Comparison between Passive and Active solar still

Passive Solar Still	Active Solar Still
Mechanical or electronic devices is not required.	Require mechanical or electronic devices to harness solar energy.
Little or no maintenance needed.	A lot of maintenance required.
External power source is not needed to operate, rely on their heat-absorbing properties, particularly the materials used in the system.	External power source required to operate.
Less control in collecting and delivery of energy.	Allows controlled and efficient collecting and delivery of energy

2.6 Factors affecting solar still's water productivity

There are also several factors affecting the production from the following aspects which are environment, design, and operation. The parameters from each aspect are shown as Figure 2.8 below.

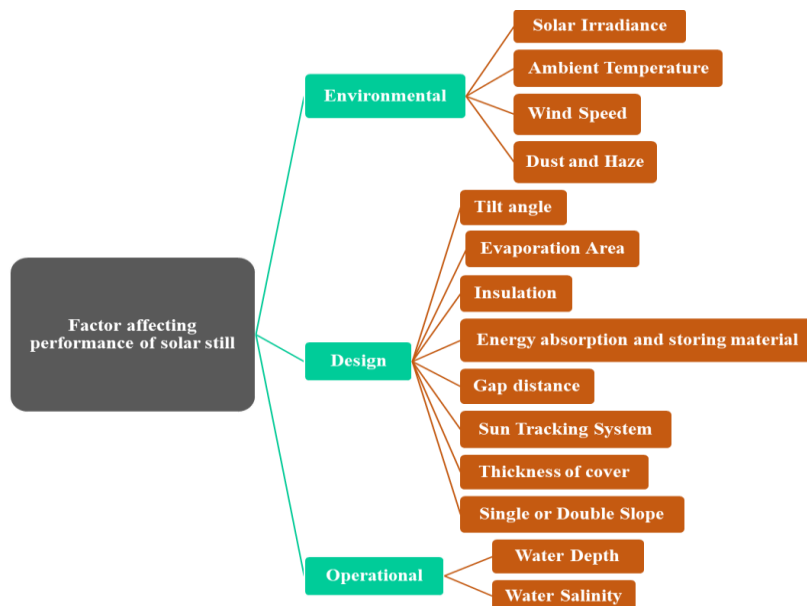


Figure 2.8: Factors influencing solar still output

2.6.1 Climatic parameters

2.6.1.1 Solar Radiation

Solar still productivity highly depend on the solar radiation. Many researchers have studied the relationship between solar radiation and productivity. Their results reflect that the distiller productivity is direct proportional to the intensity and duration of radiation which will changes with time.

2.6.1.2 Ambient temperature

Two different cases were studied from other researchers, it is found that in case 1, a drop in surrounding temperature result in increased still's output. In case 2, the reverse is seen. As an illustration, consider the following condition: lower surrounding temperature can assist in cooling down the cover quicker in order to increase the temperature difference between the water surface and the cover, however, this is only applicable on solar still equipped with good insulation; if solar still is uninsulated, low surrounding temperature will increase heat loss causing a reduction in water temperature although the cover still cooled by the

low ambient temperature, but the heat loss has greater influence than lower cover temperature.

Multiple studies using theoretical model have demonstrated that a different in 5°C enable a microscopic improvement in solar still efficiency by 3%. This theory also validated by Hinai, et al. (2002), who found that still production increase 8.2%, when the surrounding temperature rise 10°C

2.6.1.3 Wind speed

As stated by El-Sebaei. (2000), wind speed will influence the temperature of the cover by convection. The convection between the cover and surrounding increase when wind velocity higher and this will impact on the evaporation rate, condensation rate and water yield. The evaporation rate increases with the increase of wind speed as the temperature difference between the cover and water increase, as the cover temperature have been cooled down by faster wind velocity cause the condensation rate increase so productivity increase. However, to apply this concept, the solar still must be completely vapour tight as if there is a small hole, productivity of solar still will definitely decrease with the increase of wind velocity.

2.6.1.4 Haze and dust

Haze and dust on the surface of cover can greatly affect the condensation process and caused reduction in the coefficient of radiation incidents. Hence, efficiency of the solar still will also decrease. If dust get into the cover's inner surface, the water might drip down from the cover before it flows to the collecting trough. However, this is an unavoidable factor when the solar still need to place at outside to receive sunlight so frequent cleaning and checking on the cover surface is essential in order to optimize the output. (Ali, et al., 2014)

2.6.2 Design Parameter

2.6.2.1 Single and double-sloped solar still

Based on the experiments conducted by researchers in India, as a compared with DSSS, SSSS able to receive greater amount of solar radiation at both low and high latitude locations. (Garg and Mann, 1976)

Eduardo, et al. (2000) stated that, there was not obvious difference between DSSS and SSSS in productivity under similar temperature of water and cover after they conducted an experiment by controlling on the temperature of water and cover with DSSS laboratory setup and compared with SSSS experimental data.

2.6.2.2 Tilt angle

As shown in Figure 2.9 below, in different season and different type of solar still, the tilt angle showed different productivity. The tilt angle showed an important effect on the solar still. To decide on the angle, will need to take in the consideration of the cover facing direction and its latitude and inclination. It was assumed that coverings with a slope aligned with the degree of latitude will receive typical sun radiation on a regular basis. This is critical as evaporation is affected by solar irradiance. According to experiment by other researchers in Jordan (latitude 31.57°N), the output of solar still could varies by 63% alone by only adjusting the angle of cover. (Khalifa and Hamood, 1997)

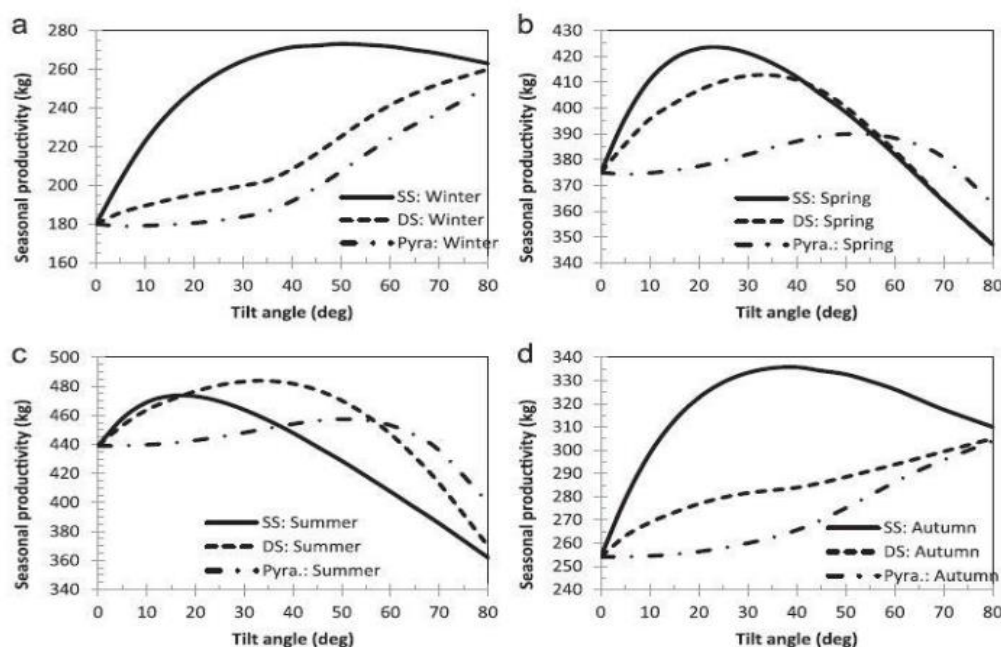


Figure 2.9: Still's productivity varies with tilt angle in different seasons

(Suresh, et al., 2017)

2.6.2.3 Thickness and material of cover

Thickness of the cover is also one of the concerns in design of solar still as when thickness increase the rate of heat transfer decrease. This is due to the heat travelled distance become longer so it required more time to heat up and more heat loss during the transmission. Moreover, Mink, et. al (1998) proved that, when a 3mm glass cover is used the water production by solar still improved by 16.5% compared to a 6mm glass cover.

Another concern is the material used for the cover. The material of the cover usually is among glass and plastics (acrylic) as choices in the design. Obviously, plastics is more cost-effective for experiment used although glass is more favourable as glass can transmit sunlight better from varies incident angle which promote long-term use.

2.6.2.4 Insulation

A study from Abdul Jabbar N. Khalifa and Ahmad M. Hamood (2009), discovered that, raising the thickness of insulation did enhance the still yield and operating temperature. When the thickness input of insulation are 30, 60 and 100mm, the night-time still's yield was enhanced to 0.45, 0.55, and 0.60L respectively compare with uninsulated still which only produce 0.20L. From the experiment, it is showed that more than 80% of impact on solar still output influenced by the thickness of insulation where the still output improved with from 1.81 L/m² to 3.28 L/m² per day with 60 and 100 mm thickness of insulation. This finding is consistent with the findings of Abu-Arbi, et al. (2002), who revealed that excellent insulation can optimize the saline water temperature by 67%. This is due to a continued output was obtained during low or no sunlight period. The effective thickness of insulation was discovered to be substantial up to 60mm and afterward it showed an asymptotic effect.

2.6.2.5 Energy absorption and storing materials

Numerous studies have been conducted to boosting incident insolation, for examples, enhancing the absorption rate of the solar still (e.g. energy supplies can be improved by adding charcoal and coal into water which can enhance the absorption rate of energy from the sun for evaporation) in turn, heat losses also reduced. The existence of absorbents enhances the thermal efficiency and water

production of solar still. The black stones absorb incoming sun's radiation better than both treated and untreated metallic wiry sponges, increasing production by about 20%. Sakthivel and Shanmugasundaram (2015) showed that, still yield improved by around 20% by adding black granite graphene as a medium of energy storage in single-basin solar still. From this result, it is observed that storage system can boost the output of still by applicable of LHS. This approach is based on the discharge of heat from the under of the basin. The adoption of PCM as storage medium is gaining popularity in current study.

2.6.2.6 Sun tracking system

Sun tracking system can help to increase solar still productivity by keep track of the movement of sun. Therefore, the position of the solar still can be modified accordingly to improve the performance of solar stills. According to Abdallah, et al. (2008), a solar tracking device has mounted on a conventional solar still with stepwise basin, was significantly increased the production by 380%.

2.6.2.7 Evaporation area

The rate of water evaporates in a solar still is also relies on the evaporation area. As mentioned earlier the water vaporization is a surface phenomenon. So, when the area of water exposed or the evaporation area increase, more water molecules will vaporize. Due to this, using a larger surface area of the basin can also boosts solar still output.

2.6.2.8 Gap distance

Gap distance represent the distance between the surface of the cover and the water surface. This gap will also bring significant impact on the performance of solar still. As claimed by Ali.F. Muftah, et al. (2014), the gap distance is far more substantial than the influence of inclination angle of the cover. In the research, it was mentioned that another researcher Ghoneyem (1995) found that a 11% increase in water production when the gap distance is reduced from 13.0 cm to 8 cm. This implies that, reducing the gap between water surface and cover surface can improve the productivity of solar still greatly. As if the gap distance is too large, when the vapour come out from the water surface will mix with air again lead to low production.

2.6.3 Operational Parameter

2.6.3.1 Water Depth

Water depth is one of the operational parameters that affecting the solar still productivity. The relationship between water depth and solar still productivity is inversely proportional. According to Elango and Kalidasa Murugave (2014) experiment, production of solar still at water depth of 1cm to 5cm were studied. As shown in Table 2.5, the maximum output occurs when water depth is 1cm and when water depth at 5cm it gives minimum output compared to 1cm to 4cm. Hence, higher water productivity can be obtained by lower the deepness of water. However, it is slightly challenging to attain the water level at minimum level constantly as dry spot will happen.

Table 2.5: Still's output by different insulation thickness (Elango and Kalidasa Murugave, 2014)

Variation in operating parameters under insulated condition.

Date	7/3/2014			11/3/2014			20/3/2014			2/4/2014			5/4/2014		
Depth of basin fluid	1 cm			2 cm			3 cm			4 cm			5 cm		
Operating condition (insulation)	Average I _s		Output	Average I _s		Output	Average I _s		Output	Average I _s		Output	Average I _s		Output
	S. B.	D. B.		S. B.	D. B.		S. B.	D. B.		S. B.	D. B.		S. B.	D. B.	
Time	(kWh/m ²)		ml	(kWh/m ²)		ml	(kWh/m ²)		ml	(kWh/m ²)		ml	(kWh/m ²)		ml
6:00 AM	0.156	0		0	0.155		0	0		0.128	0		0	0.144	
7:00 AM		0	0		0	0		0	0		0	0		0	0
8:00 AM	0.483	15	5	0.409	10	0	0.459	0	0	0.484	0	0	0.426	0	0
9:00 AM		30	20		20	15		15	5		10	0		0	0
10:00 AM	0.759	75	75	0.715	65	55	0.736	30	25	0.714	20	15	0.720	5	10
11:00 AM		160	145		135	125		65	75		35	45		25	30
12:00 PM	0.929	290	255	0.926	205	220	0.927	115	165	0.939	85	105	0.933	55	85
1:00 PM		495	415		415	370		375	305		305	210		285	145
2:00 PM	0.902	590	525	0.927	510	480	0.884	465	390	0.882	420	305	0.887	385	255
3:00 PM		560	500		500	465		430	375		395	345		315	325
4:00 PM	0.557	350	455	0.450	320	420	0.412	310	345	0.478	285	320	0.472	275	305
5:00 PM		295	430		285	375		280	335		265	300		250	290
6:00 PM	0.133	210	385	0.134	235	340	0.117	245	305	0.145	255	285	0.137	225	280
7:00 PM		155	345		165	315		200	280		205	270		215	270
8:00 PM	0	125	240	0	130	250	0	165	255	0	165	260	0	185	265
9:00 PM	0	90	205	0	95	210	0	125	220	0	135	235	0	165	255
10:00 PM	0	55	115	0	70	120	0	85	125	0	90	135	0	120	145
11:00 PM	0	40	95	0	45	105	0	60	115	0	70	120	0	90	125
12:00 AM	0	20	55	0	30	65	0	45	85	0	50	90	0	60	95
1:00 AM	0	10	35	0	20	45	0	25	60	0	30	70	0	35	75
2:00 AM	0	0	15	0	0	20	0	5	40	0	10	50	0	15	55
3:00 AM	0	0	0	0	0	10	0	0	15	0	5	20	0	10	25
4:00 AM	0	0	0	0	0	0	0	0	5	0	0	10	0	0	10
5:00 AM	0	0	0	0	0	0	0	0	0	0	0	0	0	0	5
6:00 AM	0	0	0	0	0	0	0	0	0	0	0	0	0	0	0
Total output (ml)		3565	4315		3255	4005		3040	3525		2835	3190		2715	3050
Total average radiation (kWh/m ² /day)	3.917			3.715			3.663			3.783			3.730		
Specific production (ml/kWh/m ² /day)		910	1102		876	1078		830	962		749	843		728	818

2.6.3.2 Salt concentration

Based on Kalbasi and Esfahan (2010) experiment, a 20% reduction in water production when water salinity was increased from 0% to 3.5%. Thus, the water product is strongly related to salt concentration in water and is inversely proportional. On the report of Akash, et al (2000), the effect of water salinity percentage on water production are shown in Figure 2.10 below.

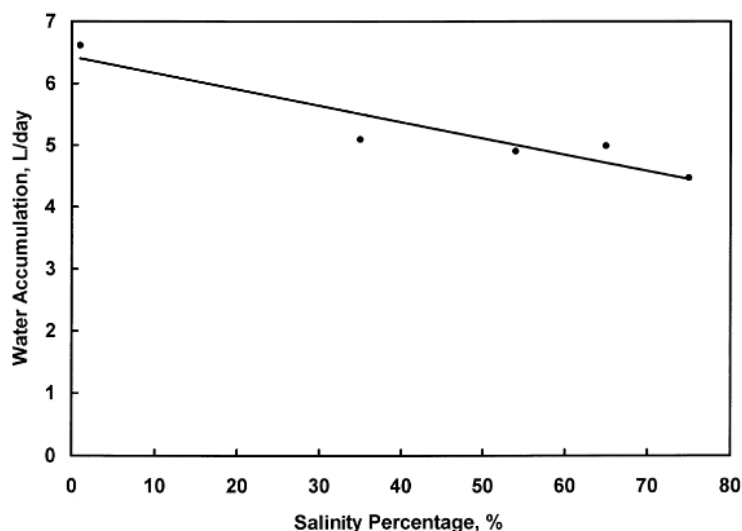


Figure 2.10: Effect of water salinity percentage on solar still productivity
(Akash, et al., 2000)

2.7 Summary

The purpose of this literature review was to gain clearer knowledge on TES system with the use of PCM. Also, to give better understanding on working principle of PCM and its characteristics and properties. Based on the research, it is known that the thermal conductivity of PCM is relatively low to provide excellent performance. Therefore, it also offers a study on improvement of PCM with nanoparticles to overcome the downside of PCM. The efficiency of the SS was affected by various aspect from design, operational and climatic. A lot of study has been conducted to determine the factors from various aspects. After comparison, organic paraffin will be mainly used in this study and nano powder such as aluminum oxide, zinc oxide, copper and copper oxide will be considering to be used in this study. A comparison and research will be done on their thermal conductivity effectiveness and cost so either one of it will be using to conduct the experiment.

CHAPTER 3

METHODOLOGY AND WORK PLAN

3.1 Introduction

In this chapter, methodology and workflow is planned to conduct the research and for the future experiment. Study conducted in previous chapter is used to scope down the range on selecting PCMs and nanoparticles.

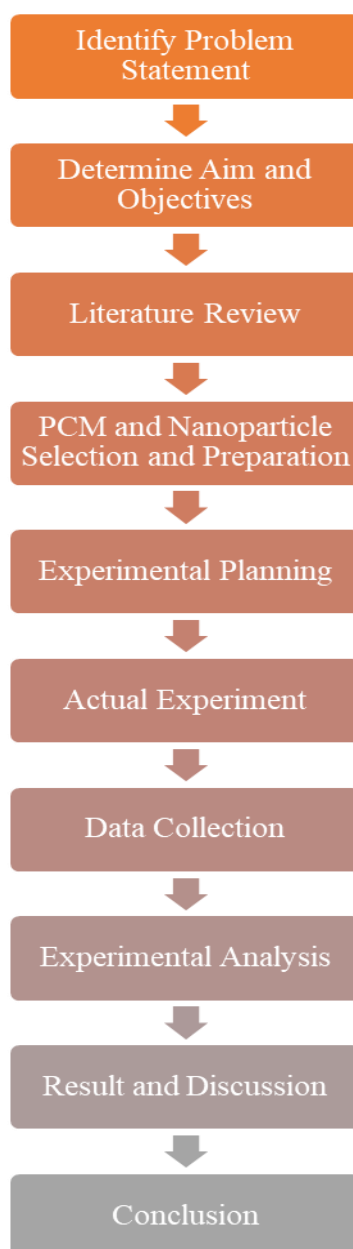


Figure 3.1: Flow chart of works

3.2 Mathematical Model of Basin Type Solar Still

According to Nguyen (2018) stated, the first studied on heat and mass transfer in a SS under ideal condition was in 1961 by Dunkle. Several assumptions have been to derive the formulae for the energy balance in the SS.

- i) Well-designed SS with no leakage
- ii) Dry air and water vapour behave as ideal gas
- iii) No heat loss
- iv) Temperature variations along the thickness of the cover and depth of water are neglected.

Figure 3.2 below demonstrates the heat and mass transfer mechanisms in a passive solar still. Solar still productivity and efficiency of solar still will be evaluated using the Equation below.

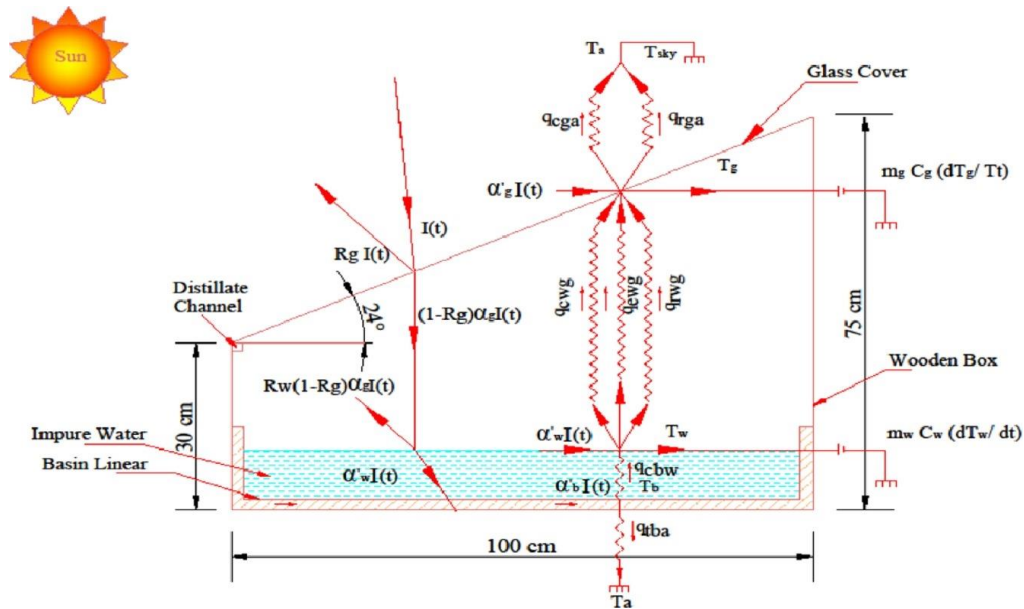


Figure 3.2: Heat transfer inside SS (Abhay, et al., 2017)

Internal heat transfer between cover and water surface:

Convective heat transfer between water and cover surface (Abhay, et al., 2017)

$$q_{twg} = 0.884 \left[(T_w - T_g) + \frac{(P_w - P_g)(T_w + 273)}{(268.9 \times 10^3) - P_w} \right]^{1/3} \quad (3.1)$$

Evaporative heat transfer between water and cover surface (Abhay, et al., 2017)

$$q_{ewg} = \frac{h_{cwg}(P_w - P_g)(16.28 \times 10^{-3})}{(T_w - T_g)} \quad (3.2)$$

where,

$$p_w = 614.17 e^{\frac{17.625 T_w}{T_w + 243.04}} \quad (3.4)$$

$$p_g = 614.17 e^{\frac{17.625 T_g}{T_g + 243.04}} \quad (3.5)$$

Radiative heat transfer between water and cover surface (Abhay, et al., 2017)

$$q_{rwg} = \frac{\varepsilon_{eff} \sigma [(T_w + 273)^4 - (T_g + 273)^4]}{(T_w - T_g)} \quad (3.6)$$

Effective emittance (El-Sebaey, et al. 2022)

$$\varepsilon_{eff} = \left(\frac{1}{\varepsilon_w} + \frac{1}{\varepsilon_c} - 1 \right)^{-1} \quad (3.7)$$

Mass Yield (Zhi, et al., 2022)

$$m_{yield} = \frac{q_{ewg}(A_w)(\Delta t)}{h_{fg,sw}} \quad (3.8)$$

Water latent heat (Zhi, et al., 2022)

$$h_{fg,w} = 2500 - 2.386 T_w \quad (3.9)$$

$$h_{fg,sw} = h_{fg,w} \times 1 - \frac{S}{1000} \quad (3.10)$$

Energy absorbed by SS (Zhi, et al., 2022)

$$E = P \Delta t \quad (3.11)$$

$$P = I(t) A_b \quad (3.12)$$

Productivity and Efficiency (Zhi, et al., 2022)

$$Productivity = \frac{\sum m_{yield}}{\sum E} \quad (3.13)$$

$$Efficiency = \frac{\sum m_{yield} h_{fg,sw}}{\sum E} \quad (3.14)$$

where

T_w = Water temperature, °C

T_g = Cover temperature, °C

q_{twg} = convective heat transfer between water and cover surface, $W/m^2\text{°C}$

q_{ewg} = evaporative heat transfer between water and cover surface, $W/m^2\text{°C}$

q_{rwg} = radiative heat transfer between water and cover surface, $W/m^2\text{°C}$

p_w = Water surface pressure, N/m^2

p_g = Cover inner surface pressure, N/m^2

ε_{eff} = emissivity of water to cover surface

ε_w = emissivity of water, 0.96

ε_c = emissivity of acrylic cover, 0.90 – 0.95

σ = Stefan Boltzman's constant, $5.67 \times 10^{-8} W/m^2K^4$

A_w = evaporation area, m^2

Δt = time difference, s

$h_{fg,sw}$ = SW latent heat of vaporization (kJ/kg)

$h_{fg,w}$ = water latent heat of vaporization (kJ/kg)

E = energy used (kJ)

P = solar power (W)

S = water salinity

m_{yield} = mass yield, g

Further, the thermal conductivity, latent heat, and specific heat of the NePCM can be calculated by formulae below. (Aziz and Abdolrahman, 2015)

$$K_{npcm} = \frac{[K_{np} + 2K_{pcm} - 2(K_{pcm} - K_{np})\phi]}{[K_{np} + 2K_{pcm} + (K_{pcm} - K_{np})\phi]} K_{pcm} + 5 \times 10^4 \beta_k \zeta \phi \rho_{pcm} C_{p_{pcm}} \sqrt{\frac{BT}{\rho_{np} d_{np}}} f(T; \phi) \quad (3.14)$$

$$C_{p_{npcm}} = [\phi(\rho C_p)_{np} + (1 - \phi)(\rho C_p)_{pcm}] / \rho_{npcm} \quad (3.15)$$

$$\rho_{npcm} = \phi \rho_{np} + (1 - \phi) \rho_{pcm} \quad (3.16)$$

$$L_{npcm} = (1 - \phi)(\rho L)_{pcm} / \rho_{npcm} \quad (3.17)$$

$$f(T; \phi) = (2.8217 \times 10^{-2} \phi + 3.917 \times 10^{-3}) \frac{T}{T_{ref}} + (-3.0669 \times 10^{-2} \phi - 3.91123 \times 10^{-3}) \quad (3.18)$$

where

K_{npcm} = thermal conductivity of NePCM, W/mK

K_{pcm} = thermal conductivity of PCM, W/mK

- K_{np} = thermal conductivity of nanoparticle, W/mK
 ϕ = volumetric fraction of nanoparticle
 β_k = $8.4407(100\phi)^{-1.07304}$
 ζ = Brownian motion correction factor, $\zeta \begin{cases} 0 & \text{if } T < T_{solids} \\ \frac{T - T_{solids}}{T_{liquids} - T_{solids}} & \text{if } T_{solids} < T < T_{liquids} \\ 1 & \text{if } T > T_{liquids} \end{cases}$
 Cp_{pcm} = specific heat of PCM, J/kg K
 B = Boltzmann constant, 1.381×10^{-23} J/K
 T = Temperature of NePCM, K
 T_{ref} = Reference temperature, K (= absolute temperature 273K)
 T_{solids} = Temperature of NePCM at solids state, K
 $T_{liquids}$ = Temperature of NePCM at liquids state, K
 ρ_{np} = density of nanoparticle, kg/m^3
 d_{np} = diameter of nanoparticle, m
 $\rho C p_{np}$ = energy density of nanoparticle, J/kg K
 $\rho C p_{np pcm}$ = energy density of NePCM, J/kg K
 $\rho_{np pcm}$ = density of NePCM, kg/m^3
 ρ_{pcm} = density of PCM, kg/m^3
 $L_{np pcm}$ = latent heat of NePCM, J/kg
 L_{pcm} = latent heat of PCM, J/kg

3.3 PCM Selection

Before selecting PCMs, it is important to make comparison between the 3 types of PCMs which are organic, inorganic and eutectic. The advantages and drawbacks of these PCMs are shown in the Table 3.1 and 3.2 below.

Table 3.1: Comparison on organic and inorganic PCMs

Properties	Impact	Organic	Inorganic
Melting temperature	Operating temperature for specific application	Available in wide range of temperature (-5°C to 190°C)	Available in wide range of temperature (18.5°C to 116°C)
High latent heat of fusion	Storage size	Lower than inorganic	Higher (125–280 J/g, low & mid range; 250–450 J/g high range)
High specific heat	Provide additional significant sensible heat storage	High	High
High thermal conductivity	Charging and discharging times	Lower than inorganic (0.314W/mK) in solid state	High (0.5W/mK)
Small volume expansion during phase transition	Reduce containment problem	Larger than inorganic	Smaller (10% more)
High density	Reduce containment size	Lower	Higher
Congruent melting	Melt congruently in order to prevent irreversible segregation.	Ability to melt congruently	Due to phase segregation, congruent melting is not achievable.
Chemical stability	PCM storage and release the heat as many times as required by an application.	Stable up to 500°C, chemically inert	Not stable, degradation occur due to phase segregation
Compatibility with other materials	Long lifetime of the vessel that contains the PCM and the other surrounding materials preventing the leakage of the PCM.	Not corrosive, Innocuous	Corrosive (PCMs can undergo degradation after serval cycle as a result of crystallization due to water loss, decomposition or chemical interaction with the containers).
No/little supercooling	Reduce the energy storage capacity	No supercooling	Supercooling is particularly a problem for salt-hydrates, and it will interfere with the extraction of energy or prevent it completely
Good crystallization and nucleation rate	The system can meet demand of heat recovery from the storage system	Possible	Not possible due to phase segregation.

From Table 3.1, it is observed that, organic PCMs is slightly advantages than the inorganic PCMs. Although inorganic PCMs posed higher thermal conductivity, lower cost and abundant which fulfil most of the ideal thermal and economic properties of PCMs listed in Figure 2.5 but from other aspect like kinetic, chemical, physical and environment is still unfavourable. Hence organic PCMs which able to fulfil most of the criteria is more favourable in this for this system. Even though the thermal conductivity of the organic PCM is comparatively lower but it's thermal conductivity can be improved by nanoparticle. The installation cost of organic PCM and inorganic PCM are comparable though starting cost of organic PCMs might be higher.

Table 3.2: Benefits and Drawbacks of 3 types of PCMs

Type of PCMs	Advantages	Disadvantages
Organic	<ul style="list-style-type: none"> - Chemically inert - No phase segregation - Thermally stable for repeated cycles - Low vapour pressure - Non-corrosive - No supercooling - Stable below 500 - Recyclable - Compatible with most materials - Self nucleating 	<ul style="list-style-type: none"> - Low thermal conductivity - Moderately flammable - Non-compatible with plastic container - Lower phase change enthalpy - High volume change
Inorganic	<ul style="list-style-type: none"> - High volumetric storage - Cheap and readily available - Non-flammable - Sharp phase change - Potentially recyclable - Higher thermal conductivity 	<ul style="list-style-type: none"> - Super-cooling - Phase segregation - Corrosive to metal, Irritant - High vapour pressure - Low durability - Moderate chemical stability - Self nucleating not possible
Eutectic	<ul style="list-style-type: none"> - Sharp melting temperature - High volumetric thermal storage 	<ul style="list-style-type: none"> - Limited data available - High cost

As mentioned in paragraph earlier, organic PCMs have greater advantages than inorganic PCMs. Therefore, another comparison is made between the organic and eutectic PCMs. Organic PCMs is more ideal material to be used in the study due to the cost of eutectic PCMs is high and there are limited data and information available in current research.

3.3.1 Data and Preparation of Organic PCMs

It is believed that Malaysia will be gradually adopt the solar energy in various application for moving towards the sustainable development goal (SDG) although it is still not widely utilized in Malaysia.

From previous study of UiTM, temperature of saline water can heat up to 73.4°C (highest) in active solar still and 60.7°C (lowest) in passive solar still. (Kamarulbaharin et.al, 2018) The difference between active and passive solar still is various type equipment (e.g., photovoltaic panel, concentrator, and thermal collector) is used to direct the solar radiation in active solar still for the desalination process while in passive solar still sunlight is directly collected in the process (Tiwari, 2007). Furthermore, from another research saline water temperature can heated up to an average of 51°C in a pyramid shape solar still (Shehabuddeen, Katyiemb and Mazhanash, 2015).

From the information above, it is note that, the PCM used in the solar still in Malaysia with a melting point below 61°C is suitable. There are 2 types of organic PCMs which are paraffin and non-paraffin. Non-paraffin PCMs is fatty acid which is either animal or plant-based oil such as palmitic acid (palm oil), lauric acid and stearic acid. Both paraffin and fatty acid exhibit equivalent properties but slightly difference in environmental effect as shown in Table 3.3 below.

Table 3.3: Difference between paraffin and fatty acids on environmental effect

Properties	Paraffin	Non-paraffin (fatty acids)
CO ₂ emissions during manufacturing	more	lesser
Non-toxicity	✓	✓
Corrosiveness	✗	Mild
Renewable	✗	✓

Moreover, as a compared to paraffin PCM, non-paraffin PCMs are more eco-friendly. However, there are always pros and cons, non-paraffin PCMs, will have mild corrosion to other material due to its natural acidic properties. According to T. Trisnadewi et al (2021), time needed for palm wax to complete 1 cycle is longer than paraffin wax. Although thermal conductivity degraation on palm wax is lesser, but the palm wax viscosity reduces as temperature increase shown in Table 3.4. Hence paraffin wax is still a better option as it has higher phase change enthalpy in cooling where energy released to the system is greater than palm wax while the cost of these waxes are similar as shown in Table 3.5.

Table 3.4: Thermal cycle test for palm and paraffin waxes (T. Trisnadewi et al, 2021)

Number of cycles	Palm wax				Paraffin wax			
	Heating		Cooling		Heating		Cooling	
	T _m (°C)	ΔH (J/g)	T _f (°C)	ΔH (J/g)	T _m (°C)	ΔH (J/g)	T _f (°C)	ΔH (J/g)
0	56.96	149.17	38.83	105.92	58.17	135.35	57.02	124.78
500	56.34	173.36	37.65	97.812	57.83	139.35	54.17	131.31
1000	56.14	164.18	37.49	92.589	59.12	136.30	55.23	133.01
3000	55.99	176.69	36.62	97.366	61.25	158.22	57.19	150.27
5000	56.06	142.35	37.27	83.326	62.25	109.59	58.73	108.19

Table 3.5: Cost comparison of PCMs

Type of PCMs used	Price (RM/kg)	Melting temperature (°C)
Paraffin wax	RM20 from SHOPEE RM5/100g	48 – 60 (Begin liquify at 40)
Palm wax	RM16.00 from SHOPEE - palm wax flake, extra processing required	50 – 60
Soft paraffin (petroleum jelly)	RM5/100g from SHOPEE	37

The properties of organic PCMs of both paraffin and non-paraffin will be listed in Table A.1 and A.2 in appendix. After comparison, the most suitable PCM will be paraffin wax. In this study, a paraffin will be the focus in this study. Soft paraffin and paraffin wax will be used to conduct the experiment.

3.4 Nanoparticles Selection

In previous study, it is found that there are 2 methods to enhance the PCMs. However, adding additives (nanoparticles) in PCMs is more favourable in this study as still lack of information on nanoencapsulation in this field and this method required high production cost and purification treatment is needed.

Adding nanoparticles to PCMs, would be a more convenient approach. This method can also effectively improve the charging and discharging speed which represent the melting rate and solidification rate of PCMs.

3.4.1 Data and Preparation of nanoparticles

After understanding on the preferable type of nanoparticle are, carbon-based, metal and metal oxide based on this study. It is also the common type of nanoparticle used to mix with PCMs for enhancing its thermal conductivity. Comparison on the thermal conductivity of various type nanoparticle and its' prices were listed in Table 3.6.

Table 3.6: Comparison on nanoparticle price and thermal conductivity

Nanopowders	Thermal conductivity (W/mK)	Cost (RM)	Quantity (g)	Size (nm)
Aluminum Oxide (Al ₂ O ₃)	40	83.25/60.31	100	10-20/30
Zinc Oxide (ZnO)	22	78.49/58.82	100	20/40
Tin Oxide (SnO ₂)	36	314.64	100	50
Iron Oxide (Fe ₂ O ₃)	7	104.88/91.77	100	30/50
Titanium Dioxide (TiO ₂)	8.5	72.10	100	20
Copper Oxide (CuO)	33	98.32/88.49	100	20/50
Carbon nanotubes (>95/97wt%)	3000 (Multi-walled) 6000 (Single-walled)	196.48 196.48/642.22	10 1	<8 1-2/<2
Zirconium (IV) Oxide (ZrO ₂)	2.2	91.77	100	20
Silicon nitride (Si ₃ N ₄)	29 – 30	456.88/371.67	100	20/50
Boron nitride (BN)	30 – 33	138.97	100	100
Yttrium oxide (Y ₂ O ₃)	27	203.20	100	20
Aluminium (Al)	239			
Copper (Cu)	386	281.86	10	50
Aluminum nitride (AlN)	140 – 180	268.76	100	40
Diamond nanopowder (C)	900	-	-	-
Silver nanopowder (Ag)	424	137.66/537.51	10/50	-
Graphene	3000 – 5000	589.78	0.5	~2
Silicon dioxide (SiO ₂)	10.4	79.97	100	20
Silicon carbide (SiC)	490	371.67	100	50
Magnesium Oxide (MgO)	48.4	117.10	100	30

From Table 3.6 above, nanoparticles with relatively high thermal conductivity are very expensive such as, graphene, copper, silicon carbide, silver and carbon nanotubes. As from economic aspect, these nanoparticles will not be choosing in this study. To consider both cost and thermal conductivity of the nanoparticles, aluminium oxide, magnesium oxide or zinc oxide would be more suitable for the experiment thus either one of them will be used to conduct the experiment.

3.5 Design of PCM storage

Concept of single slope solar still will be used in this study. The design of the single slope solar still in this study is shown as Figure 3.2.

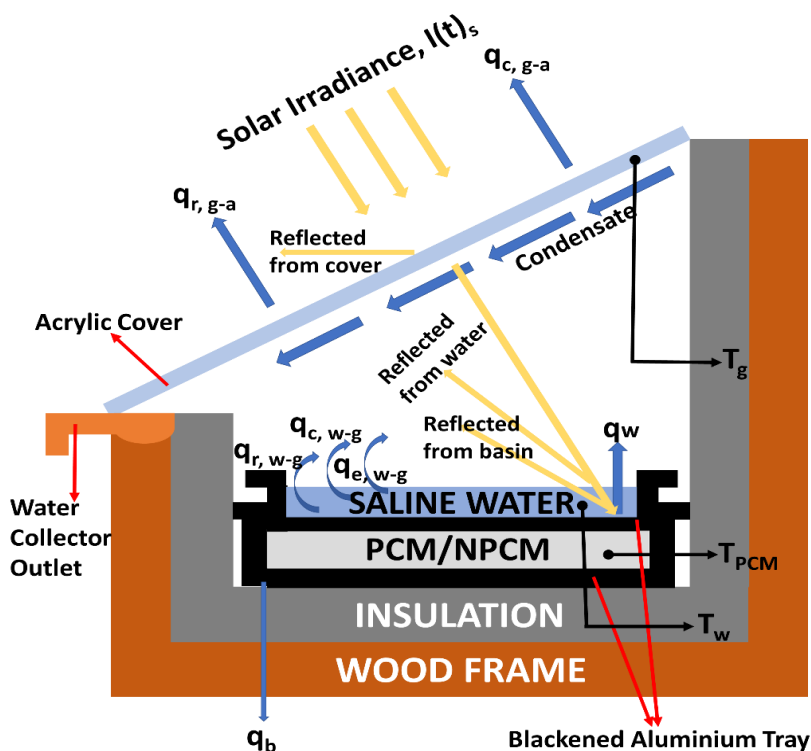


Figure 3.3: Design of single slope solar still in this study

A small and simple solar still model will be built for the experiment as in this study, it is mainly focus on the performance of PCM and nanoparticle. First, 2 similar sizes of aluminium tray as shown in Figure 3.3, the upper aluminium tray will contain the saline water while the bottom aluminium tray will be containing PCM/NePCM. The bottom aluminium tray will be slightly larger than the upper one. Then the smaller aluminium tray will put on the larger one and the gap will be sealed by silicone sealant to prevent leakage of PCM. An acrylic cover will be used.

Both aluminium tray will be painted black to absorb sunlight better. Furthermore, a 3mm acrylic cover will be used and with an inclination of 18°, the wood frame will be using plywood and MDF.

3.6 Experiment Planning

Before the experiment start, fabrication of solar still model and purchasing on material were completed. There are 2 different PCM were used in this study.

- i. Pure paraffin wax
- ii. Pure soft paraffin (petroleum jelly)

The first experiment will be comparing between solar still which are without PCM, with paraffin wax, and with soft paraffin wax to observe which would give a better performance and higher efficiency. In first experiment, 3 similar small solar still model will be placed at outdoor under the sun or places where sunlight will not block by buildings or trees to make sure it able to absorb solar energy to heat the water inside. The PCM that give higher efficiency and water productivity will then use to mix with aluminium scrap and disperse with nano powder to conduct the following experiments.

After the first experiment, the second experiment will be comparing the solar still with pure PCM and PCM with aluminium scrap (1-2wt%) to find out if additive of high thermal conductivity substances able to enhance weakness of PCM on thermal conductivity. After that, solar still with PCM with aluminium scrap and PCM with nano powder (1wt%) will be comparing in the third experiment to investigate whether both of it bring equivalent effect. Similarly, the second and third experiments will repeat what have done in the first experiment but with different model. To mix the PCM with aluminium scrap and nano powder, hotplate with magnetic stirrer is used to melt the PCM. Step of preparation of PCM with nanoparticle is showed as Figure 3.4 below.

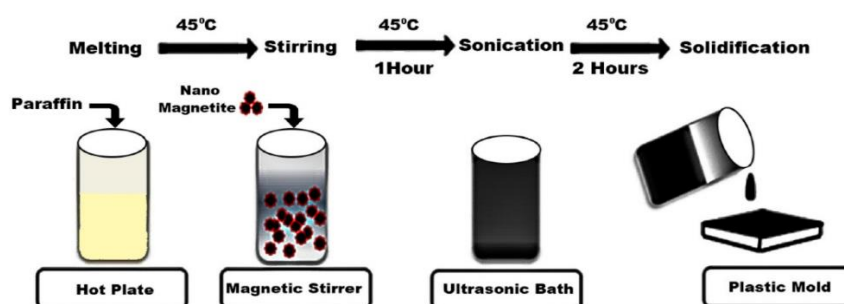


Figure 3.4: Procedure of preparing PCM with nanoparticle. (Al-Yasiri and Szabó, 2021)

Further, saline water was also prepared for the experiment. Multiple type-K thermocouples will connect to several point inside the solar still to obtain the temperature of water, cover, PCM and surroundings in every 1 hours. The experiments were conducted in Desa Petaling, Kuala Lumpur, Malaysia. In every 1 hour, measurements of solar irradiance, water temperature and yield, glass temperature and ambient temperature will be taken. The experiment will be conducted from 10a.m. to 5a.m.

CHAPTER 4

RESULTS AND DISCUSSION

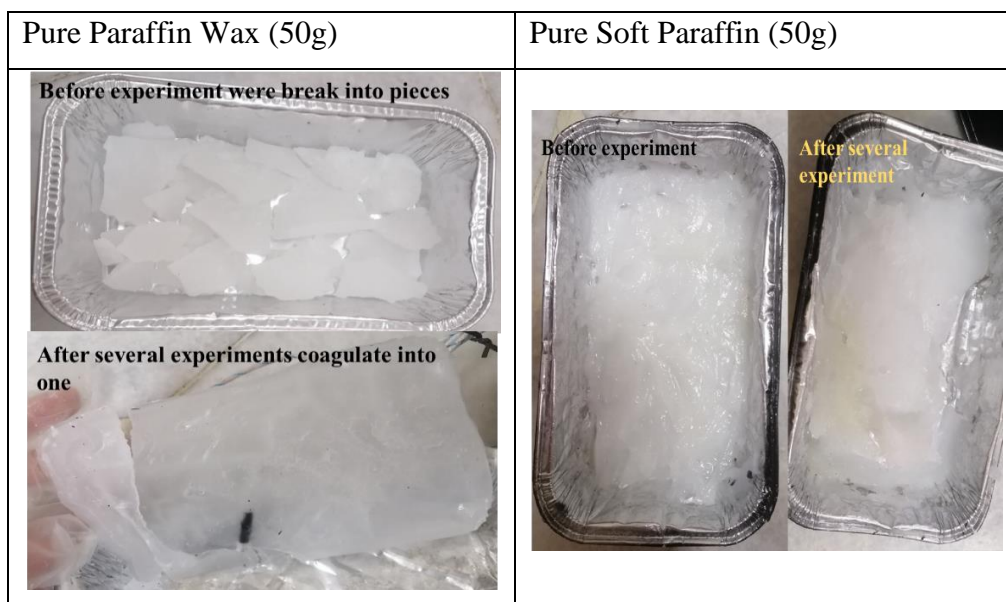
4.1 Introduction

In this chapter, the experiment result will be discussed and presented. The data of the experiment was thoroughly examined and analysed in order to gain a deeper insight of how PCM enhances the water production of solar stills and how nano particle improve the thermal conductivity and performance of PCM.

4.2 Experiment

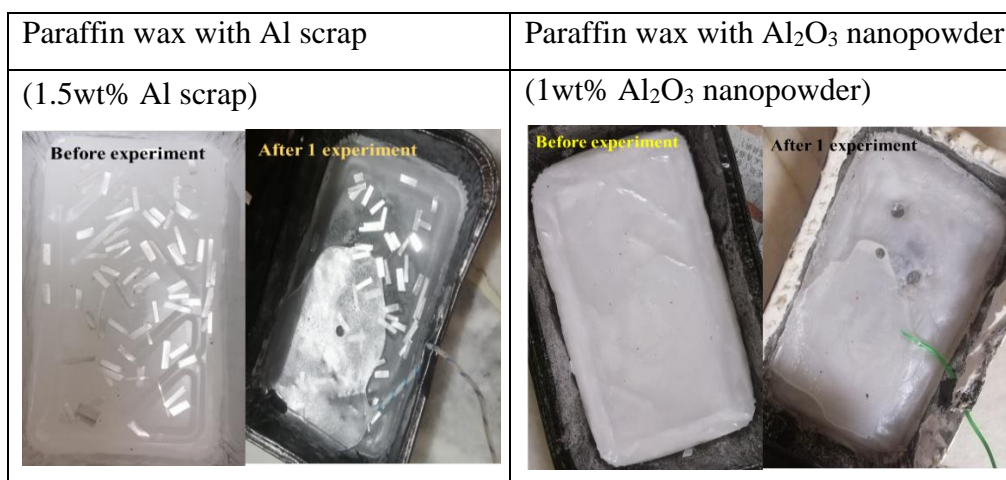
The PCM used in the experiment is shown in Figure 4.1 and 4.2 below. The first experiment was only using pure paraffin wax and pure soft paraffin (petroleum jelly) to investigate which of the PCM have performance.

Figure 4.1: Condition of PCMs before and after experiments



After several round of repeated experiments, it were showed that pure paraffin wax gave higher efficiency and productivity as a compare to pure soft paraffin, so the pure paraffin wax will be using to conduct the second experiment, another two 50g of paraffin wax will be melted and mix with 1.5wt% aluminium scarp and 1wt% alumina nanopowder each.

Figure 4.2: Condition of NePCMs before and after experiments



Initially the pure paraffin wax was come as a square block, hence it was broken into pieces and filled into the bottom aluminium tray which is the PCM container to conduct the experiment. After several cycle, it is observed that the pure paraffin wax was melted and coagulated into one whole rectangle block. This indicate that, paraffin wax undergoes phase transition in order to coagulate into 1 as shown in Figure 4.2. This implies the theory, where heat energy is absorbed when solid is melting into liquid and energy is stored during the phase change which also known as latent heat. When the substances are crystalline from liquid to solid, heat is release. Unlike the pure paraffin wax just break into pieces, the paraffin wax with additive (aluminium scrap or Al₂O₃ nanopowder) will need to undergo a series of procedure stated as previous chapter.



Figure 4.3: Experiment setup



(upper left corner: model with paraffin wax, middle: model without PCM, upper right corner: model with soft paraffin)

Figure 4.4: Prototype of Solar Still with tilt angle at 19°

Figure 4.3 above showed the experiment setup and Figure 4.4 showed the prototype of solar still used in this experiment. Due to the prototype is small the design of the solar still is simpler. The water depth is 1cm in every experiment and the gap distance between the water surface and cover inner surface is 6cm for all models. The whole wood frame of the solar still was wrapped with waterproof self-adhesive PVC wallpaper. Then the inner wall of the wooden frame will also stick on another layer of XPE foam act as insulation to prevent heat received loss to surroundings. The cover of the solar still will temporarily seal by tape when conducting the experiment. 3 model is built as to conduct the experiment of different model at the same time order to make comparison under the same weather condition. Refer to appendix for the specification of solar still.

4.3 Temperature

The temperature of water, PCM, acrylic cover and surroundings play a vital role in this study. As these temperatures have determined how much energy have received, charging and discharging process of PCM, performance of different PCM, heat transfer between saline water and PCM in solar still, relationship

between the solar irradiance and temperature of water, PCM and cover. These parameters are crucial for this study to evaluate the performance of latent thermal storage via PCM.

4.3.1 Experiment on PCM effects

Graphs below showed the temperature measured during the experiments.

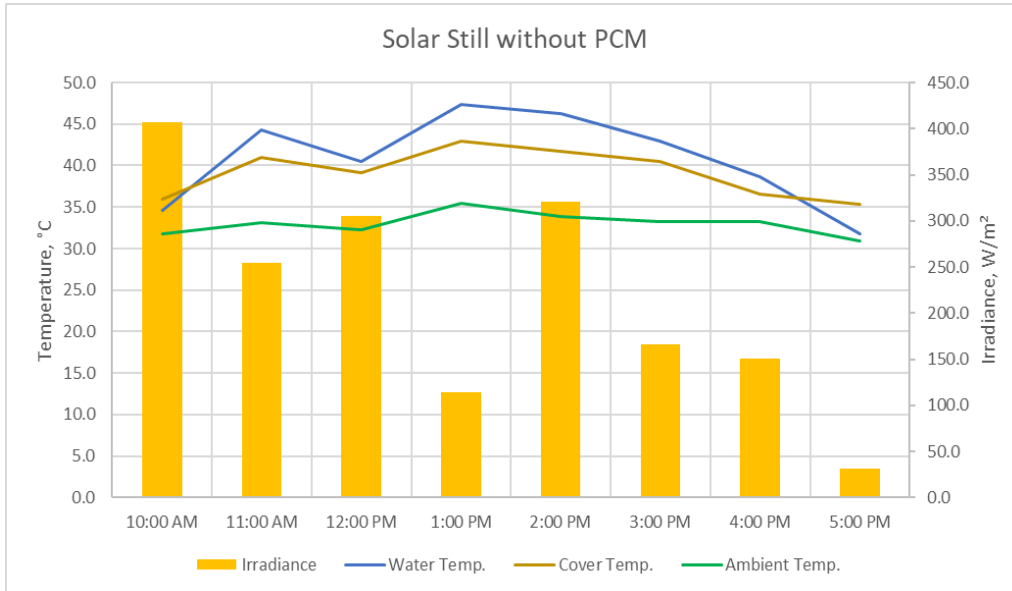


Figure 4.5: Graph of SS without PCM (model A)

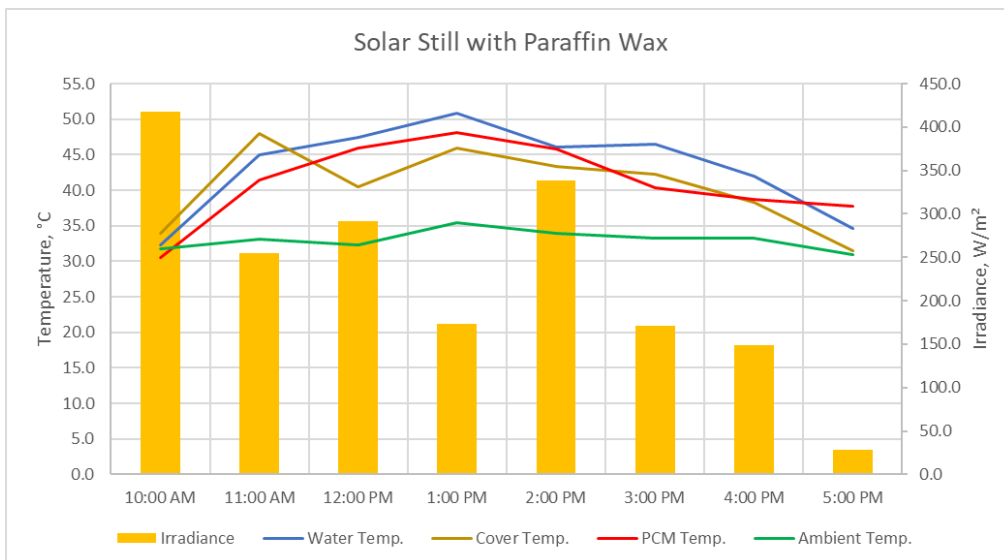


Figure 4.6: Graph of SS with Paraffin wax (model B)

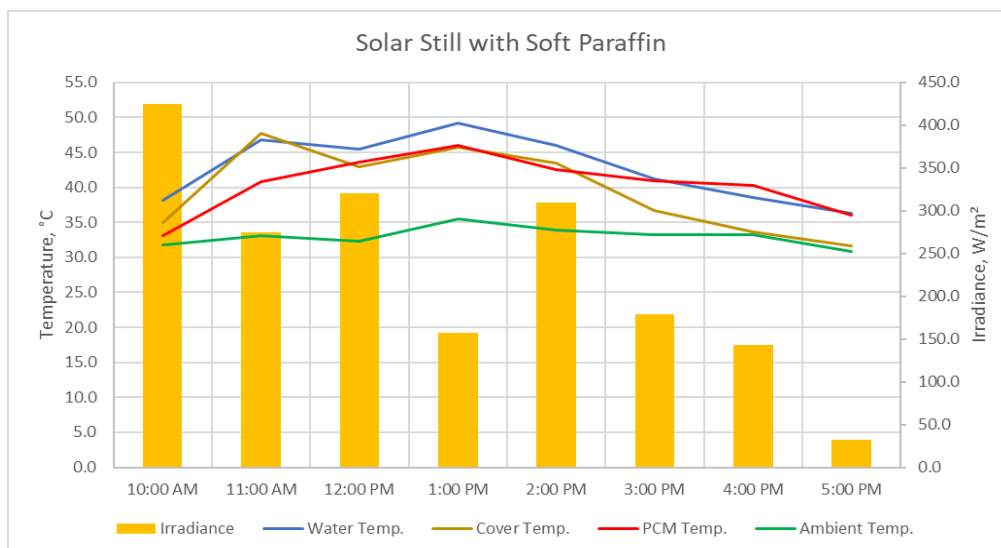


Figure 4.7: Graph of SS with Soft paraffin (model C)

From Figure 4.5, it is observed that the relationship between the temperature of saline water and solar irradiance is directly proportional. When solar irradiance rise, saline water temperature higher. When solar irradiance decreases, saline water temperature also decrease. This prove that the principal of radiation heat transfer of solar still where heat energy is transmitted in the forms of rays to the solar still as heat energy is absorbed and slowly heat up the saline water causing evaporation as when water receive sufficient energy, it will evaporate at any temperature. There are more water molecules with higher kinetic energy at higher temperature, thus more water evaporates.

According to Figure 4.6 and 4.7 above, the temperature of water in solar still with paraffin wax or soft paraffin were higher than the solar still without PCM. The feed temperature has a sharp increase from 10:00 a.m. to 11:00 a.m. and gradually increase from 11:00 a.m. to 1:00 p.m. and come to its peak at 1:00 p.m. After that, the water temperature is slowly decrease from its peak. The maximum solar Irradiance received by model A, B and C were 407.1, 417.6, 424.4 W/m² respectively at 10:00 a.m. The maximum water temperature reached by model A, B and C were 47.3, 50.9 and 49.2°C at 1:00p.m. respectively and the average temperature difference between the cover and water surface were 2.89, 3.80, and 3.30°C respectively. Furthermore, the maximum PCM temperature occurred in model B and C were 48.1 and 46.0°C at 1:00p.m. respectively. According to the study in chapter 2, for solar still with

insulation the increment in difference between water and cover surface will lead to an increment on evaporation and condensation rate in order to provide higher productivity. Hence, model with highest average temperature difference between water and cover have the highest productivity.

Based on Figure 4.5 and 4.6, the graph showed that paraffin wax having longer heating time this is due to the melting point of it is higher while soft paraffin seems to heat up faster and discharge at the earlier stage. As observed in the graph, soft paraffin starts to discharge at around 3:30p.m. to around 5:00p.m. the temperature of soft paraffin was slightly lower than the water temperature which mean that the soft paraffin can no longer supply heat to the water. In contrast, paraffin wax has a longer heating duration, it starts to discharge at around 4: 30p.m and will constantly discharging afterward.

Due to the weather condition, the experiment have to be stopped at 5:00 p.m. However, it can be predicted and assumed that the discharging time of paraffin wax will be slightly longer than that of soft paraffin as the charging time of paraffin wax was longer which mean more heat were stored and the temperature difference between water and paraffin wax were smaller than temperature difference between water and soft paraffin. This indicate that, thermal conductivity of paraffin wax is better although it has a higher melting point as during the charging period most of the heat were able conduct from water to it under same condition with soft paraffin. Also, according to water yield of SS with paraffin wax was slightly higher than that of soft paraffin hence paraffin wax was using for the next experiment.

4.3.2 Experiment on PCM enhanced by nanoparticle

After comparing on the PCM, another experiment were done on the improvement for PCM to enhanced it's thermal conductivity to increase the solar still output. Figure 4.8 and 4.9 below showed the graph of SS with pure paraffin wax and SS with paraffin wax with aluminium scrap.

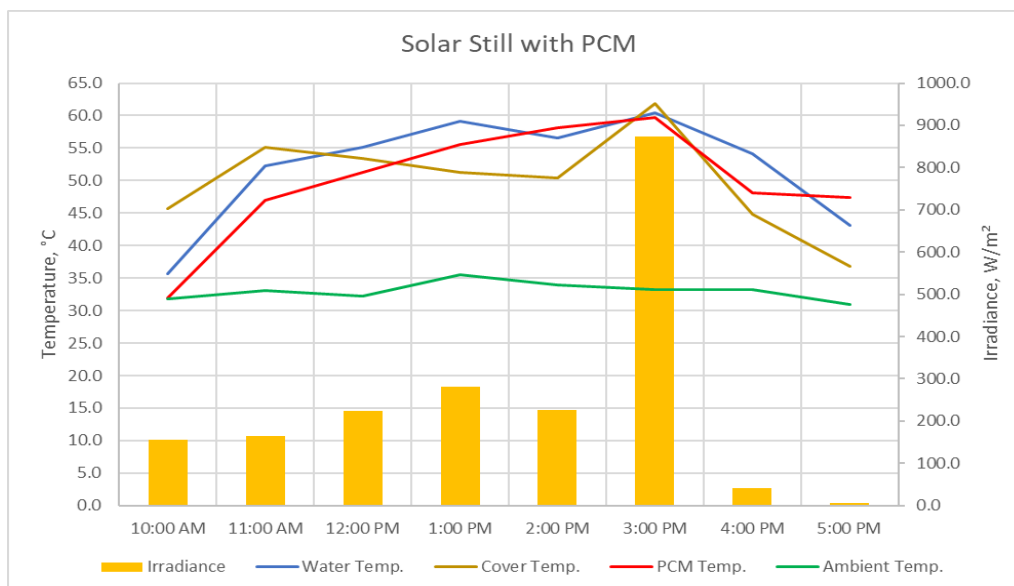


Figure 4.8: Graph of SS with Paraffin wax (model B)

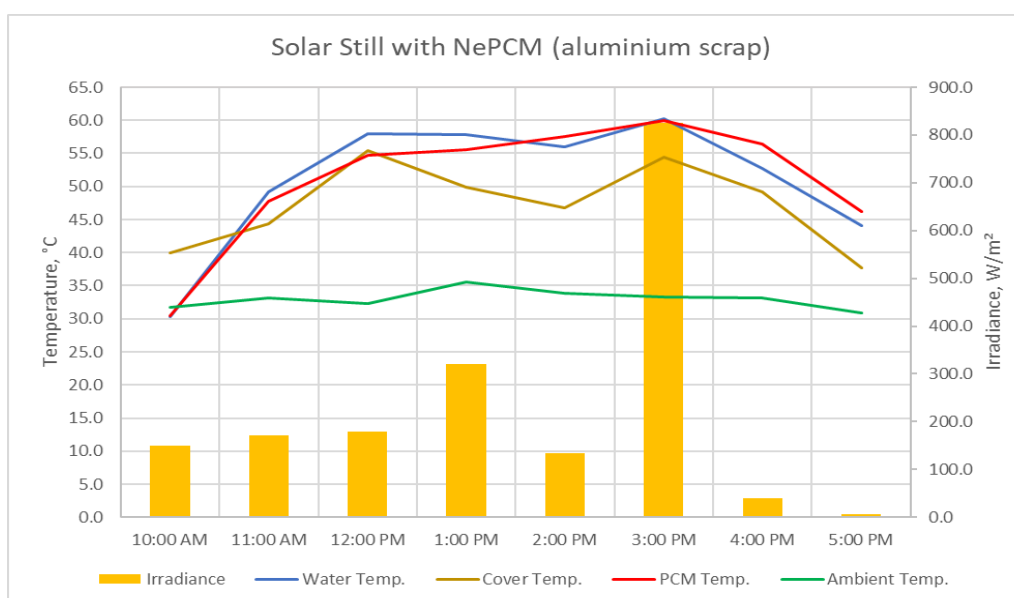


Figure 4.9: Graph of SS with Paraffin wax with Al scrap (model D)

From both of the graph above, the solar irradiance of all day seems to be quite low, the solar irradiance was gradually increase from 10:00a.m. to 1:00p.m. and slightly drop at 2:00p.m. However, solar irradiance was sharply increased to the peak of the day at 3:00 p.m. and drop drastically at 4:00 p.m. then slowly without sunlight. This is due to the weather sometimes cloudy sometimes sunny from 10:00 a.m. to 3.00 p.m. and the drastic drop from 3:00 p.m. to 4:00 p.m. was owing to heavy clouds which was a sign of raining. Therefore, again the experiment stops at 5:00 p.m.

It was observed that the temperature curve of paraffin wax containing aluminium scrap showed a smoother curve. The feed temperature has a sharp increase from 10:00 a.m. to 11:00 a.m. and gradually increase from 11:00 a.m. to 3:00 p.m. and come to its peak at 3:00 p.m. After that, the water temperature started to decrease from its peak and decrease acutely from 4:00 p.m. to 5:00 p.m. in model B and in model D, it decreases smoother from its peak to the end of the experiment. The maximum solar irradiance received by model B and D were 872.6 and 826.0W/m² respectively at 10:00 a.m. and average solar irradiance were 246.7 and 228.6W/m² throughout the experiment, respectively.

The maximum water temperature achieved by model B and D were 60.4 and 60.2°C at 3:00p.m. and the average temperature difference between the cover and water surface of both models were 5.7 and 6.3°C respectively. The maximum PCM temperature reached by model B and D were 59.7 and 60.0°C at 3:00p.m. respectively.

By observing the temperature of PCM and water it was noted that, the temperature of NePCM with Al scrap was smoother and very close to the water temperature while the temperature of pure paraffin wax has greater different. The discharge process occurred when the PCM temperature higher than the water temperature, from the graph, it was known that the SS with NePCM containing Al scrap started discharged at around 1:30 p.m. and continuously discharging until the end of the experiment. On the other hand, SS with pure PCM also started a noticeably short discharging duration at the same time but only maintained around 1 hours, and started another discharge around 4:30 p.m. So, obviously, NePCM with Al scrap exhibit better thermal conductivity than that of PCM as the NePCM with aluminium scrap receive heat energy close to the water as shown by the temperature difference between water and PCM and improving the rate of production as observed by water yield in every 1-hour further details will showed in water productivity section.

As a result, addition of high thermal conductivity material to PCM could improve the thermal conductivity of PCM and improve the production rate accordingly.

4.3.2.1 Comparison on aluminium scrap and alumina nano powder

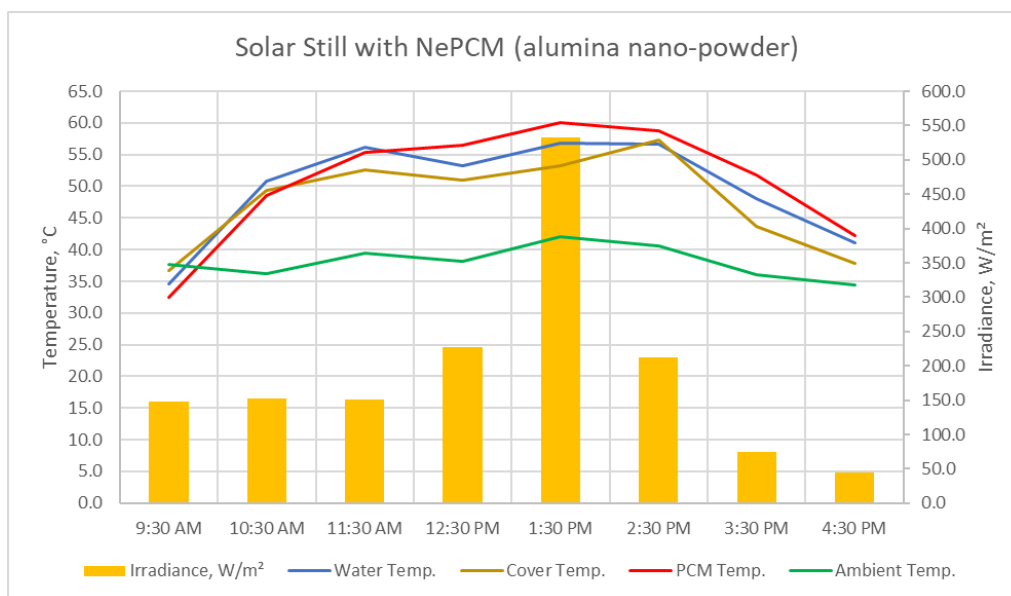


Figure 4.10: Graph of SS with Paraffin wax with Al₂O₃ nanopowder (model E)

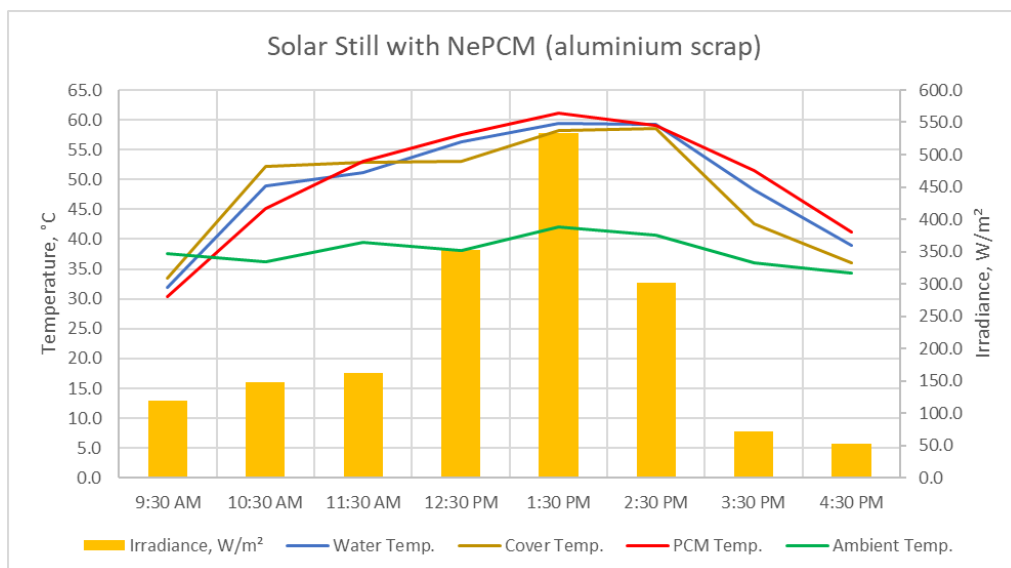


Figure 4.11: Graph of SS with Paraffin wax with Al scrap (model D)

The experiment was conducted to evaluate whether Al scrap can replace the nano powder to give the same amount of efficiency. Again, the solar irradiance was gradually increase from 9:30a.m. to 11:30a.m. and increase acutely from 11:30 a.m. to its peak at 1:30 p.m. After that, it was sharply decrease from 1:30 p.m. to 3:30 p.m. and slowly decrease again.

It was observed that the temperature curve of both models showed a smoother curve. The feed temperature has a sharp increase from 9:30 a.m. to 10:30 a.m. and gradually increase from 10:30 a.m. to 1:30 p.m. and come to its peak at 1:30 p.m. After that, the water temperature started to decrease from its peak smoothly from 2:30 p.m. to 4:30 p.m. The maximum solar irradiance received by model E and D were 533.0W/m^2 for both at 1:30 a.m. and average solar irradiance received were 192.8 and 217.7W/m^2 respectively. The maximum water temperature achieved by model E and D were 56.8 and 60.6°C at 1:30p.m. respectively and the average temperature difference between the cover and water surface were 2.7 and 2.6°C respectively. The maximum PCM temperature reached by model E and D were 60.0 and 61.9°C at 1:30p.m. respectively.

By observing the temperature of PCM and water it was noted that, both of the temperature of NePCM obtained a smooth curve and very close to the water temperature while the temperature of pure paraffin wax has greater different. Based on the graph, it was shown that, the model D PCM started discharged at around 11:00 a.m. and continuously discharging until 2:00p.m. and discharge again at around 2:45p.m. Similarly, model E NePCM also started discharging at around 11:30 a.m. which is about 30 minutes later than model D PCM however it was able to consistently releasing energy to the water until the end of the experiment as nano-particle have reduced the time required for paraffin wax to complete one cycle of charge and discharge hence it able to continuous supply energy to water. As a compare with pure paraffin wax, the time required on charging was double than that of the NePCM.

In short, the temperature difference between the cover and water surface determined the evaporation and condensation rate while the nanoparticle bring a significant effect on reducing the time required for PCM to complete one cycle of charge and discharge in order to improve water production.

4.4 Water productivity and Solar Still Efficiency

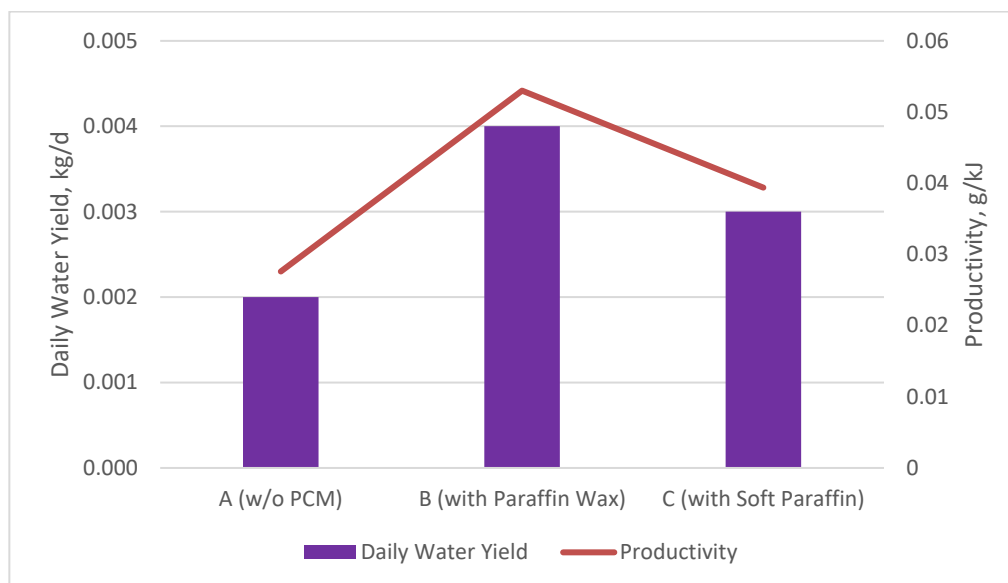


Figure 4.12: Daily water yield and water productivity of Model A, B, C

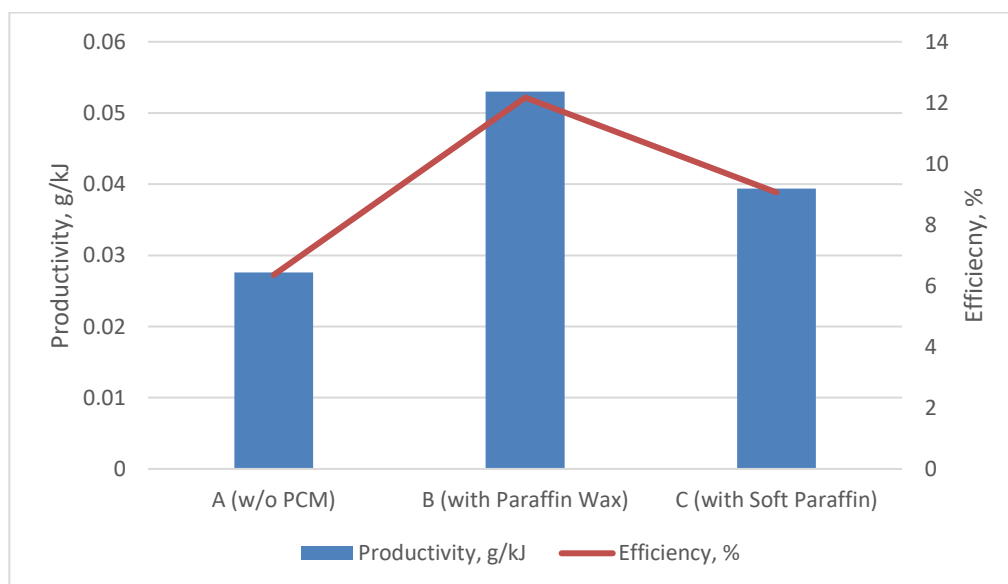


Figure 4.13: Water productivity and SS efficiency of Model A, B, C

Table 4.1: SS efficiency of model A, B, C

Model	Daily Water Yield, kg/d	Energy (E), kJ	Productivity, g/kJ	Efficiency, %
A (w/o PCM)	0.002	72.459	0.028	6.360
B (with Paraffin Wax)	0.004	75.464	0.053	12.173
C (with Soft Paraffin)	0.003	76.197	0.039	9.058

Due to the size of the solar still is relatively small, the water yields were also very little. SS without PCM only able to produce 0.002 kg/d while SS with paraffin wax and soft paraffin were producing 0.004kg/d and 0.003kg/d, respectively. The solar still with paraffin wax as thermal storage provide a better performance in productivity and efficiency. It's improved the efficiency of solar still without PCM by 5.81% and 3.11% higher efficiency than solar still with soft paraffin. This indicate that paraffin wax possesses better thermal conductivity and higher high capacity throughout the experiment.

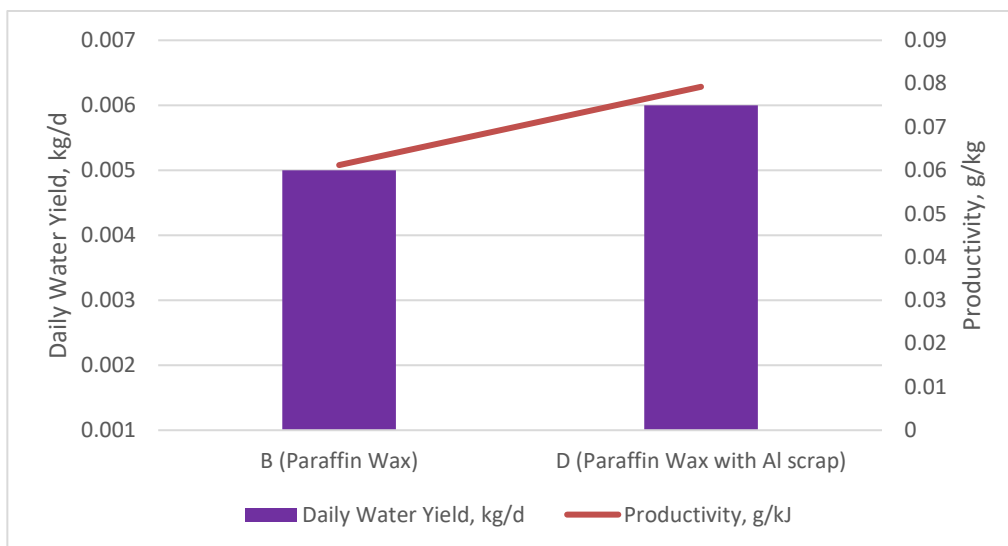


Figure 4.14: Daily water yield and water productivity of Model B and D

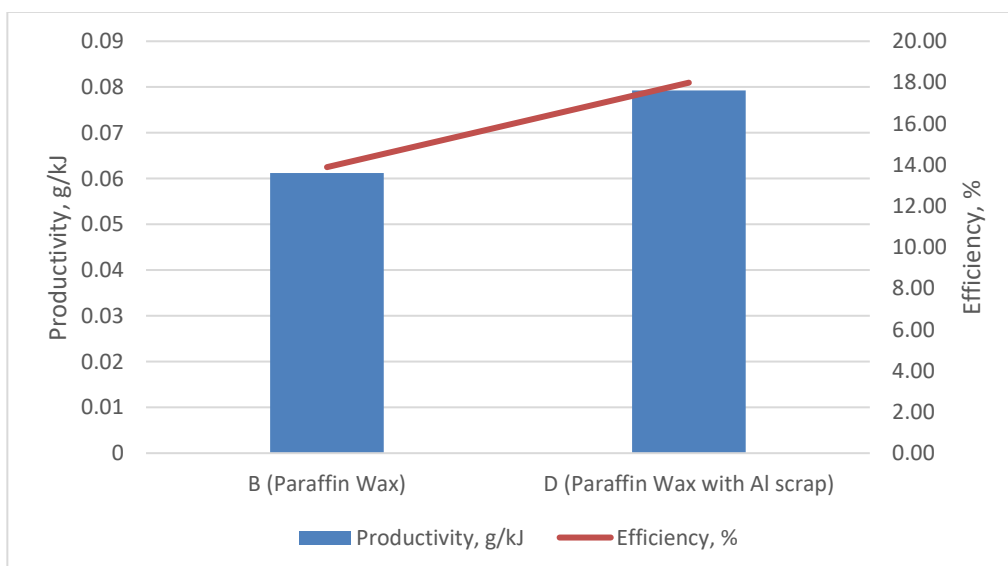


Figure 4.15: Water productivity and SS efficiency of Model B and D

Table 4.2: SS efficiency of model B and D

Model	Daily Water Yield, kg/d	Energy (E), kJ	Productivity, g/kJ	Efficiency, %
B (Paraffin Wax)	0.005	81.702	0.0612	13.890
D (Paraffin Wax with Al scrap)	0.006	75.692	0.079	17.990

For the experiment between model B and D, SS with pure paraffin wax was able to produce 0.005 kg/d while SS with paraffin wax containing Al scrap were producing 0.006kg/d. The solar still with paraffin wax containing Al scrap did improved the water productivity and SS efficiency. It's improved the efficiency of solar still with pure PCM by 4.10%. This shows that paraffin wax with additive of high thermal conductivity material can improved it thermal conductivity and help in production rate.

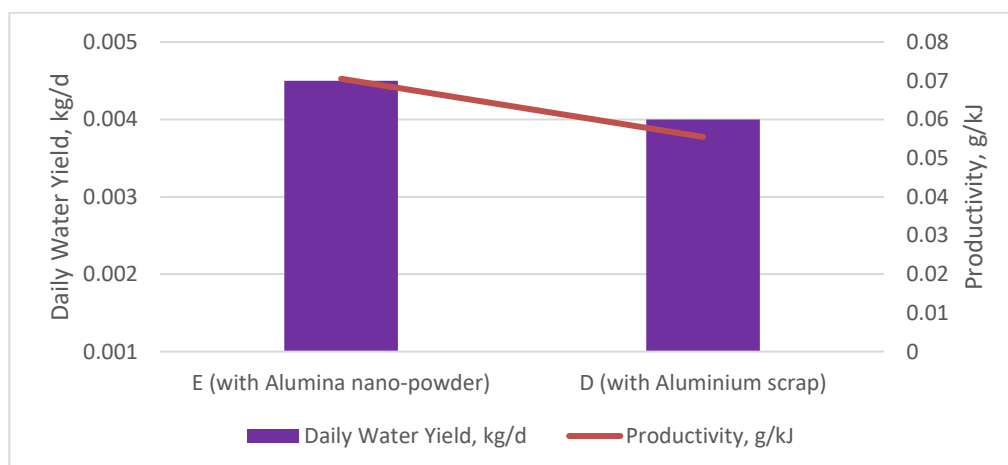


Figure 4.16: Daily water yield and water productivity of Model E and D

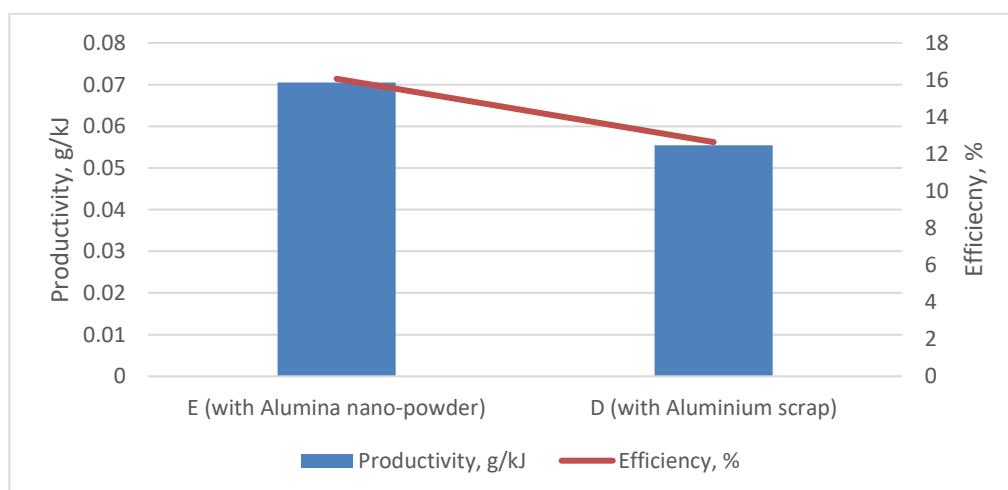


Figure 4.17: Water productivity and SS efficiency of Model E and D

Table 4.3: SS efficiency of model E and D

Model	Daily Water Yield, kg/d	Energy (E), kJ	Productivity, g/kJ	Efficiency, %
E (with Alumina nano-powder)	0.005	63.829	0.071	16.066
D (with Al scrap)	0.004	72.099	0.055	12.645

Table 4.3 showed, model E SS was 3.42% higher efficiency than the model D. the water yield by model E was 0.005 kg/d while model D SS was 0.004kg/d. There are only 0.001 kg/d difference of water yield between the 2 model, but the energy required for modal E solar still to produce 0.005kg/d was lesser than that of model D. Also, there are 1.5wt% of aluminium scrap in paraffin wax (model D) while there is only 1wt% of alumina powder in paraffin wax (model E) but the water yield by model E are still 0.001kg/d greater than model D so the model E efficiency is definitely higher but it can also predict that if 3.0wt% of aluminium scarp is use in model D it might similar production rate as 1wt% of Al_2O_3 nano powder in model E.

Therefore, the efficiency of model E is higher. This is due to smaller particle promote a faster rate on heat transfer. However, the result showed on the model E productivity was not as expected as compared to another research. This might be due to the lack of procedure when mixing the nanoparticle and paraffin wax which will be further discuss in section 4.7 below. This is also the reason aluminium scrap was used to conduct the experiment. Due to this reason the experiment between model E and D can only take as a reference but it is not enough to prove the SS efficiency with NePCM (containing the alumina nano powder) but it was believed that if with proper procedure on mixing the nanoparticle the efficiency will definitely better than what have been obtained in this experiment.

4.5 Water Conductivity



Figure 4.18: TDS value of water before and after experiment

Theoretically, water distilled from solar still is safe to drink hence to prove the water is safe to drink, a water conductivity test should be carried out. From the Table 4.4 below, the TDS value of water before and after experiment were tabulated. Before the experiment, the TDS value of water is 10800 ppm which is extremely higher than 1000ppm and is not safe to drink but after the experiment the water TDS value is only 65 which mean it is safe to drink. As according to the Figure A.1 in appendix A, water safe for consumption should below 500ppm and over 1000ppm are definitely cannot process by human body.

Table 4.4: TDS values of water before and after experiment

	Before experiment	After experiment
Total Dissolved Solids (TDS) in ppm	10800	65

4.6 Cost Analysis

Table 4.5: Cost analysis on PCM

Material	Cost, RM/100g	Mass used, g	Water Yield, g	Cost per water yield, g/RM
Paraffin wax	5.00	50.00	4.00	1.60
Soft paraffin	5.00	50.00	3.00	1.20

From Table 4.5 showed, paraffin wax is more cost - effective than soft paraffin. As shown as above, with RM 1, 1.6g of water can be produced by solar still with paraffin wax as thermal storage while 0.4g lesser of water is produce by solar still with soft paraffin. As the solar still built to conduct the experiment is small so the water yield is very less due to small evaporation area, therefore with a larger solar still with paraffin wax, RM 1 can produce more water than what have presented.

Besides that, there are another 2 experiments conducted between SS with pure paraffin wax (model B) and SS with aluminium scrap (model D) and between SS with Paraffin wax containing aluminium scrap (model D) and SS with paraffin wax mixing nanoparticle (model E). The water yield difference between model B and D is 0.001kg while model D and E is 0.001kg, hence it can be estimated that difference between model B and E is 0.002kg.

Table 4.6: Cost analysis on nanoparticle

Material	Cost, RM/100g	Mass used, g	Water Yield, g	Cost per water yield, g/RM
Pure paraffin wax	5.00	50.00	5.00	2.00
Al scrap + Paraffin wax	0 + 5.00	0.75+50.00	6.00	2.40
Alumina nano powder + Paraffin wax	60.31 + 5.00	0.50 + 50.00	7.00	2.50

Refer to Table 4.6 above, model E can produce 2.5g of water in RM.1 while pure paraffin wax only able to produce 2g of water in RM 1. Additionally, the payback period of the solar still with or without PCM and NePCM can be calculated as below (Deepti Charitar1 and Amos Madhlopa, 2008):

$$n_{pb} = \frac{\ln\left[\frac{m_{yield} \times S_{p,w}}{(m_{yield} \times S_{p,w}) - (P_c \times i_r)}\right]}{\ln(1+i_r)} \quad (4.1)$$

$$P_c = C_{rm} + C_{labour} + C_{land} + C_{operating} \quad (4.2)$$

where

n_{pb} = *payback period*

$S_{p,w}$ = *water price*

m_{yield} = *mass yield by solar still, kg*

i_r = *interest rate*

P_c = *Capital cost*

C_{rm} = *material cost*

C_{labour} = *labour cost*

C_{land} = *land cost*

$C_{operating}$ = *operating cost (transportation cost etc.)*

Assumed that, there is 5% interest rate, the water price in Malaysia RM2.62/250ml, material cost as show in Table B.6 in appendix is RM56.50, labour cost is 30% of the material cost, operating cost, and land cost set to zero. The payback period of the solar still without PCM, with pure PCM and NePCM (aluminium scarp w PCM and alumina nano powder with PCM) are 158, 149, 145 and 142 days, respectively.

4.7 Challenges

The challenge encountered in this study was mainly on the climate change. The experiments were done on close to the rainy season which is in the mid to the end of August. As a consequent, the weathers were sometimes cloudy and sometimes sunny which might cause some inaccuracy in measurement on solar irradiance as when the measurement was taking the sunlight might covered by cloud but afterward the cloud might move away.

As what have been studied in earlier research, the solar still efficiency was highly relies on the solar irradiance, therefore, the PCM thermal storage efficiency is also relies on the solar intensity which is the main energy source of the system. However, this is an uncontrollable factor and therefore, what can do to avoid is by checking on the weather forecast before the experiment although the forecast might not always accurate.

Besides that, there's also another challenge on mixing the nano powder with the paraffin wax. According to finding on the procedure of dispersing

nanoparticle to PCM, the paraffin wax was melted by a hotplate magnetic stirrer at range of 47 to 80°C which is at its melting point or above it until it completely in liquid state then the nanoparticle can pour into the liquid state paraffin wax which will take about 1 hours. After that, a probe sonicator will be needed to stir the mixture at constant temperature that can keep the paraffin wax in liquid state for around 2 hours. To perform better heat transfer, sonication is needed to prevent agglomeration that could decline the viscosity and thermal conductivity and performance by supplying high shear force created from the ultrasonic cavitation in order to break agglomerate particle to smaller and uniform size.

However, UTAR does not have sufficient equipment to conduct the sonication process, this might cause some inaccuracy with the experiment result on PCM with nanoparticle. To minimize the agglomeration issue without the probe sonicator, the paraffin wax of 50g was divided into 2 portion to mixed with the nano powder. This mean that, the first 25g of paraffin wax will put in aluminium tray and melt it by the hotplate stirrer, and the other 25g will be melt in a small beaker. Then 0.25g of nano powder will be added into each set of paraffin wax. To avoid the particle sink only at the bottom, the solution will be stirred manually every 15 mins. Paraffin wax can congeal fast once it was taken off from the hotplate especially when there is very small amount. After 1-2 hours, the paraffin wax in aluminium tray will take off from the hot plate first after it was freeze, the mixture in small beaker will poured on it.

Alternately, ultrasonic bath (ultrasonic cleaner) which is available in UTAR but the result might not as good as mixing it using probe sonicator and the nanoparticle might coagulated in the body and at the bottom. This might be due to the water level outside the beaker does not higher than the solution inside the beaker. Therefore, the force only applied up to the solution body which is same level with water. Hence, by using an ultrasonic bath to disperse the nanoparticle need to be more careful as unlike probe sonicator give a direct contact to the solution, it is indirect contact with the solution thus it is necessary to make sure the water level outside the beaker is higher than the solution inside the beaker but not higher than the beaker. In a consequence, the nanoparticle can disperse uniformly in the solution by using ultrasonic bath. However, this process required more time which will need take up to 4 hours, thus it is not choosing to disperse the nanoparticle in this experiment due to time constraint.

CHAPTER 5

CONCLUSIONS AND RECOMMENDATIONS

5.1 Conclusions

From this study and experiments, it is proven that nano-particles able to enhance the thermal conductivity of PCM effectively with certain range of concentration. Nanoparticles enhance the thermal conductivity of PCM by reducing the time necessary for PCM to undergo a complete charge or discharge. On the other hand, discharge time should be increased.

- The experiment result is considered as consistently fair with some uncontrollable factor such as the weather and wind, which would be sometimes cloudy and sometimes sunny on the experiment day.
- Paraffin wax possess better thermal conductivity than soft paraffin and provide a 3.11% higher in efficiency.
- Aluminium scrap as a replacement of alumina nano-powder did improve the solar still efficiency by 4.10% and give higher water productivity.
- As a compare with nano-powder, the water productivity and solar still efficiency with PCM with aluminium scrap was still lower than the PCM with alumina nano-powder and it was estimated that 3.0wt% of aluminium scarp can give similar efficiency as 1wt% of alumina nano powder but this result and estimation can only take as a reference, as lack of sonication process when mixing the nanoparticle with PCM will lead to agglomeration which will declined the thermal conductivity of nanoparticle consequently affect the performance of PCM on charging and discharging time.
- A cost analysis has been conducted to evaluate the economic viability on the performance of solar still with the aid of nanoparticle in PCM. The result showed that for SS with NePCM containing alumina nano powder, SS with NePCM containing aluminium scrap and SS with pure PCM can produce 2.5g, 2.4g and 2.0g of water in RM 1 respectively. The payback period of the solar still without PCM, with pure PCM and

NePCM (aluminium scrap w PCM and alumina nano powder with PCM) are 158, 149, 145 and 142 days, respectively.

- The problems encountered in this experiment was mainly on the weather and lack of equipment and time on processing the nanoparticle. The weather can greatly affect the solar incident whereas lack of equipment on processing nano powder with paraffin wax will affect and declined the thermal performance causing the efficiency lower than expected.
- The objectives of this research were achieved on determined the suitable PCM which showed that paraffin wax will be more suitable than soft paraffin in this experiment and verified on the performance of nanoparticle assisted phase change material in solar desalination system which showed a 7.52% (4.1% increase in SS efficiency with PCM with Al scrap compare to pure paraffin while 3.42% improve in SS efficiency with PCM and alumina nano powder compare to PCM with Al scrap) increase in overall efficiency. The evaluation on the economic viability of the solar still is based on the calculated payback period and cost analysis showed in this study. Last but not least, the optimum conductive nano powder that chosen to conduct in this study was based on the comparison from other researcher's experiment and findings with considering on the nano powder efficiency and economic viability.

5.2 Recommendations for future work

To further improve the thermal conductivity of PCM and solar still efficiency, dispersion of higher thermal conductivity particles such as copper and silver should be used or the insertion of fibrous materials such as carbon fibres or nanofibers. Besides that, surfactants which can make nanoparticle more miscible by reducing the surface tension of PCM and nanoparticle. Hence, it can also be used in mixing the nanoparticle and PCM to increase the stability of the NePCM for long-term usage by chemical dispersion. Otherwise, altering the PCM materials would be another effective way to improve the efficiency, considering the economic viability.

From the aspect of design, tilt angle, insulation, storage material, basin surface area (evaporation area) and height difference between cover and water

surface and would be the main concern. Fresnel lens and solar tracker can also be added to concentrate the sunlight and adjust the solar still accordingly with the sun's movement to assist the solar still efficiency. On another aspect in operation, using a data logger to record and collect the temperature data would be more convenient and give better accuracy as it can measure and record temperature systematically as well as when retrieving and analysing data. It can help to avoid all sort of measurement and human error as measuring manually the temperature might sometimes fluctuate and it is difficult to get the most exact temperature of the substances. Therefore, with the data logger, the problem stated can be solved as it can measured the temperature systematically in every minute or even by second.

REFERENCES

A.A. El-Sebaai, 2000, Effect of wind speed on some designs of solar stills. *Energy Conversion and Management*, [e-journal] 41(6), pp.523-538. [https://doi.org/10.1016/S0196-8904\(99\)00119-3](https://doi.org/10.1016/S0196-8904(99)00119-3).

Abdul J.N.K., Ahmad M.H., 2009. Effect of insulation thickness on the productivity of basin type solar stills: An experimental verification under local climate. *Energy Conversion and Management*, [e-journal] 50(9), pp.2457-2461. <https://doi.org/10.1016/j.enconman.2009.06.007>.

Abhay A., R.S. Rana, Pankaj K.S., 2017. Heat transfer coefficients and productivity of a single slope single basin solar still in Indian climatic condition: Experimental and theoretical comparison. *Resource-Efficient Technologies*, [e-journal] 3(4), pp.466-482. <https://doi.org/10.1016/j.rffit.2017.05.003>.

Algarni, M., Alazwari, M. and Safaei, M., 2021. Optimization of Nano-Additive Characteristics to Improve the Efficiency of a Shell and Tube Thermal Energy Storage System Using a Hybrid Procedure: DOE, ANN, MCDM, MOO, and CFD Modeling. *Mathematics*, [e-journal] 9(24), p.3235. <https://doi.org/10.3390/math9243235>.

Al-harashsheh, M., Abu-Arabi, M., Mousa, H. and Alzghoul, Z., 2018. Solar desalination using solar still enhanced by external solar collector and PCM. *Applied Thermal Engineering*, [e-journal] 128, pp.1030-1040. [10.1016/j.applthermaleng.2017.09.073](https://doi.org/10.1016/j.applthermaleng.2017.09.073).

Ali. F. M., M.A. Alghoul, Ahmad F., M.M. Abdul-Majeed, K. Sopian, 2014. Factors affecting basin type solar still productivity: A detailed review. *Renewable and Sustainable Energy Reviews*, [e-journal] 3, pp.430-447. <https://doi.org/10.1016/j.rser.2013.12.052>.

Babazadeh, H., Sheremet, M., Mohammed, H., Hajizadeh, M. and Li, Z., 2020. Inclusion of nanoparticles in PCM for heat release unit. *Journal of Molecular Liquids*, [e-journal] 313, p.113544. <https://doi.org/10.1016/j.molliq.2020.113544>.

Cabeza, L., Zsembinszki, G. and Martín, M., 2020. Evaluation of volume change in phase change materials during their phase transition. *Journal of Energy Storage*, [e-journal] 28, p.101206. <https://doi.org/10.1016/j.est.2020.101206>.

Deepti C., and Amos M., n.d., *Effect of nanoparticle size on the thermo-economic performance of basin type solar stills*. Energy Research Centre, Department of Mechanical Engineering, University of Cape Town. Available at: <<https://az659834.vo.msecnd.net/eventsairwesteuprod/production-confsa-public/5ae2cd19a9644930a397cca29b3daedd>> [Accessed 09 September 2022].

Dinesh, K.C., 2008. *Thermal Energy Storage System Design & Optimization*. [pdf] India: International Journal of Engineering Science and Computing, Available at: <<https://ijesc.org/upload/2d06f6488f839624eda1ac179041e98a.Thermal%20Energy%20Storage%20System%20Design%20&%20Optimization.pdf>> [Accessed 23 April 2022].

Eanest Jebasingh, B. and Valan Arasu, A., 2020. A comprehensive review on latent heat and thermal conductivity of nanoparticle dispersed phase change material for low-temperature applications. *Energy Storage Materials*, [e-journal] 24, pp.52-74. <https://doi.org/10.1016/j.ensm.2019.07.031>.

Eanest Jebasingh, B. and Valan Arasu, A., 2020. A detailed review on heat transfer rate, supercooling, thermal stability, and reliability of nanoparticle dispersed organic phase change material for low-temperature applications. *Materials Today Energy*, [e-journal] 16, p.100408. <https://doi.org/10.1016/j.mtener.2020.100408>.

Encyclopedia Britannica. 2022. *Water Scarcity | Description, Mechanisms, Effects, & Solutions*. [online] Available at: <<https://www.britannica.com/topic/water-scarcity>> [Accessed 23 April 2022].

Encyclopedia Britannica. 2022. *Water Scarcity Facts and Statistics*. [online] Available at: <<https://www.britannica.com/story/water-scarcity-facts-and-statistics>> [Accessed 23 April 2022].

Enescu, D., Chicco, G., Porumb, R. and Seritan, G., 2020. Thermal Energy Storage for Grid Applications: Current Status and Emerging Trends. *Energies*, [e-journal] 13(2), p.340. <https://doi.org/10.3390/en13020340>.

Eng.Mohamed F. A. M., 2018. Study Of Solar Brackish Water Desalination For Domestic Applications Study Of Solar Brackish Water Desalination For Domestic Applications. M.Sc. Suez University. Available at: <<https://doi.org/10.14741/ijcet/v.8.5.2>. > [Accessed 09 September 2022].

Frigione, M., Lettieri, M. and Sarcinella, A., 2019. Phase Change Materials for Energy Efficiency in Buildings and Their Use in Mortars. *Materials*, [e-journal] 12(8), p.1260. <https://doi.org/10.3390/ma12081260>.

Ghoneyem. A, 1995., *Experimental study on the effects of the cover and numerical prediction of a solar still output*. PhD. Middle East Technical University. Available at: <<https://open.metu.edu.tr/handle/11511/9631>> [Accessed 09 September 2022].

Hirschey, J.R.; Kumar, N.; Turnaoglu, T.; Gluesenkamp, K.R.; and Graham, S., 2021. Review of Low-Cost Organic and Inorganic Phase Change Materials with Phase Change Temperature between 0°C and 65°C (2021). In: USDOE (United States Department of Energy), International High Performance Buildings Conference at 2020 Herrick Conferences, West Lafayette, Indiana, United States of America, 23-27 May 2021. Indiana, United States of America.

Jeff. W., 2021. *What are total dissolved solids?* [online] , 19 December. Available at: <https://www.wahlwater.com/What-are-Total-Dissolved-Solids_b_42.html> [Accessed 09 September 2022].

Jouhara, H., Żabnieńska-Góra, A., Khordehgah, N., Ahmad, D. and Lipinski, T., 2020. Latent thermal energy storage technologies and applications: A review. *International Journal of Thermofluids*, [e-journal] 5-6, p.100039. <https://doi.org/10.1016/j.ijft.2020.100039>.

Kalbasi R., and Esfahan M. N., 2010. Multi-effect passive desalination system, an experimental approach. *World Applied Science Journal*;[e-journal] 10(10), pp.1264–71.

Kamarulbaharin, Z.A., Safie, M.A, Azmi, A.M, Singh, B.S.B., 2018. Experimental Investigations on the Performance of a Single Slope Solar Still Coupled with Shallow Solar Pond under Malaysian Conditions. *International Journal of Engineering & Technology*, [e-journal] 7(4.26), p.159. <https://doi.org/10.14419/ijet.v7i4.26.22158>.

Krishna J. K., Vikrant P. K., Sandip S. D., 2022. An evaluation for the optimal sensible heat storage material for maximizing solar still productivity: A state-of-the-art review. *Journal of Energy Storage*, [e-journal] 50 (2022), p.104622. <https://doi.org/10.1016/j.est.2022.104622>.

Kokorina, A., Ermakov, A., Abramova, A., Goryacheva, I. and Sukhorukov, G., 2020. Carbon Nanoparticles and Materials on Their Basis. *Colloids and Interfaces*, [e-journal] 4(4), p.42. <https://doi.org/10.3390/colloids4040042>.

Lee, H., Jeong, S., Chang, S., Kang, Y., Wi, S. and Kim, S., 2016. Thermal Performance Evaluation of Fatty Acid Ester and Paraffin Based Mixed SSPCMs Using Exfoliated Graphite Nanoplatelets (xGnP). *Applied Sciences*, [e-journal] 6(4), p.106. <https://doi.org/10.3390/app6040106>.

Li, Z., Lu, Y., Huang, R., Chang, J., Yu, X., Jiang, R., Yu, X. and Roskilly, A., 2021. Applications and technological challenges for heat recovery, storage, and utilisation with latent thermal energy storage. *Applied Energy*, [e-journal] 283, p.116277. <https://doi.org/10.1016/j.apenergy.2020.116277>.

Magendran, S., Khan, F., Mubarak, N., Vaka, M., Walvekar, R., Khalid, M., Abdullah, E., Nizamuddin, S. and Karri, R., 2019. Synthesis of organic phase change materials (PCM) for energy storage applications: A review. *Nano-Structures & Nano-Objects*, [e-journal] 20, p.100399. <https://doi.org/10.1016/j.nanoso.2019.100399>.

Mahmoud S.El-S., Asko E., Ahmed H., and Hitesh P., 2022. Experimental study and mathematical model development for the effect of water depth on water production of a modified basin solar still. *Case Studies in Thermal Engineering*, [e-journal] 33(2022), pp.101925. <https://doi.org/10.1016/j.csite.2022.101925>.

Mamand, S., 2021. Thermal Conductivity Calculations for Nanoparticles Embedded in a Base Fluid. *Applied Sciences*, [e-journal] 11(4), p.1459. <https://doi.org/10.3390/app11041459>.

Muntadher M.A. S., Dhafer M.H., and Hassanain G.H., 2019. Numerical Investigation for Single Slope Solar Still Performance with Optimal Amount of Nano-PCM. *Journal of Advanced Research in Fluid Mechanics and Thermal Sciences*, [e-journal]. 63(2), pp.302-316.

Nadezhda S. B. and Mikhail A. S., 2020. Effect of Nano-Sized Heat Transfer Enhancers on PCM-Based Heat Sink Performance at Various Heat Loads. *Multidisciplinary Digital Publishing Institute*, [e-journal]. *Nanomaterials*; 10(1):17. <https://doi.org/10.3390/nano10010017>

Nazari S., M., Caggiano, A., Mankel, C. and Koenders, E., 2020. A Comparative Study on the Thermal Energy Storage Performance of Bio-Based and Paraffin-Based PCMs Using DSC Procedures. *Materials*, [e-journal] 13(7), p.1705. <https://doi.org/10.3390/ma13071705>.

Nematpour Keshteli, A. and Sheikholeslami, M., 2019. Nanoparticle enhanced PCM applications for intensification of thermal performance in building: A review. *Journal of Molecular Liquids*, [e-journal] 274, pp.516-533. <https://doi.org/10.1016/j.molliq.2018.10.151>.

Nguyen, B. T., 2018. Factors Affecting the Yield of Solar Distillation Systems and Measures to Improve Productivities. *Desalination and Water Treatment*, [e-journal] 2018. 10.5772/intechopen.75593.

Qudama Al-Y., and Márta S., 2021. Paraffin As a Phase Change Material to Improve Building Performance: An Overview of Applications and Thermal Conductivity Enhancement Techniques. *Renew Energy Environmental Sustain*, [e-journal]. 6(38). P.13. <https://doi.org/10.1051/rees/2021040>.

Raam Dheep, G. and Sreekumar, A., 2014. Influence of nanomaterials on properties of latent heat solar thermal energy storage materials – A review. *Energy Conversion and Management*, [e-journal] 83, pp.133-148. <https://doi.org/10.1016/j.enconman.2014.03.058>.

Raja E., Talal A., Sofiene M., Gaber A.E.A., Salem A., Lioua K., 2022. Experimental investigations on thermophysical properties of nano-enhanced phase change materials for thermal energy storage applications. *Alexandria Engineering Journal*, [e-journal] 61(9), pp.7037-7044, <https://doi.org/10.1016/j.aej.2021.12.046>.

Rashidi, S., Karimi, N., Mahian, O. and Abolfazli Esfahani, J., 2018. A concise review on the role of nanoparticles upon the productivity of solar desalination systems. *Journal of Thermal Analysis and Calorimetry*, [e-journal] 135(2), pp.1145-1159. <https://doi.org/10.1007/s10973-018-7500-8>.

Reddy, K., Mudgal, V. and Mallick, T., 2018. Review of latent heat thermal energy storage for improved material stability and effective load management.

Journal of Energy Storage, [e-journal] 15, pp.205-227. <https://doi.org/10.1016/j.est.2017.11.005>.

Safaei M.R., Goshayeshi H.R., Chaer I., 2019. Solar Still Efficiency Enhancement by Using Graphene Oxide/Paraffin Nano-PCM. *Energies*, [e-journal]; 12(10):2002. <https://doi.org/10.3390/en12102002>

Sarbu, I. and Sebarchievici, C., 2018. A Comprehensive Review of Thermal Energy Storage. *Sustainability*, [e-journal] 10(1), p.191. 10.3390/su10010191.

Sarı, A. and Karaipekli, A., 2009. Preparation, thermal properties and thermal reliability of palmitic acid/expanded graphite composite as form-stable PCM for thermal energy storage. *Solar Energy Materials and Solar Cells*, [e-journal] 93(5), pp.571-576. <https://doi.org/10.1016/j.solmat.2008.11.057>.

Sharshir, S., Elsheikh, A., Edreis, E., Ali, M., Sathyamurthy, R., Kabeel, A., Zang, J. and Yang, N., 2019. Improving the solar still performance by using thermal energy storage materials: A review of recent developments. *DESALINATION AND WATER TREATMENT*, [e-journal] 165, pp.1-15. <https://doi.org/10.5004/dwt.2019.24362>.

Sharma, S., Kitano, H., and Sagara, K. 2004. Phase Change Materials for Low Temperature Solar Thermal Applications. [pdf] Japan: Mie University. Available at: <https://www.eng.mie-u.ac.jp/research/activities/29/29_31.pdf> [Accessed 23 April 2022].

Shchukina, E., Graham, M., Zheng, Z. and Shchukin, D., 2018. Nanoencapsulation of phase change materials for advanced thermal energy storage systems. *Chemical Society Reviews*, [e-journal] 47(11), pp.4156-4175. <https://doi.org/10.1039/C8CS00099A>.

Shehabuddeen, K., Al Katyiem, H. H. and Mazhanash, H. (2020) Efficient Water Recycling through Solar Distillation, *Journal of Advanced Research in Fluid Mechanics and Thermal Sciences*, 15(1), pp. 17–24.

Soibam, J., 2017. Numerical Investigation of a heat exchanger using Phase Change Materials (PCMs) For small-scale combustion appliances. MSc. Norwegian University of Science and Technology. Available at: <https://www.researchgate.net/publication/324274438_Numerical_Investigation_of_a_heat_exchanger_using_Phase_Change_Materials_PCMs_For_small-scale_combustion_appliances> [Accessed 23 April 2022].

Sonker, V., Chakraborty, J., Sarkar, A. and Singh, R., 2019. Solar distillation using three different phase change materials stored in a copper cylinder. *Energy Reports*, [e-journal] 5, pp.1532-1542. <https://doi.org/10.1016/j.egy.2019.10.023>.

Nuo Y., S.W. Sharshir, Guilong P., A.E. Kabeel, 2016. Factors affecting solar stills productivity and improvement techniques: A detailed review. *Applied Thermal Engineering*, [e-journal] 100, pp.267-284. <https://doi.org/10.1016/j.applthermaleng.2015.11.041>.

T. Elango, K. Kalidasa Murugavel, 2015. The effect of the water depth on the productivity for single and double basin double slope glass solar stills. *Desalination*, [e-journal] 359(2015), pp.82-91 .<https://doi.org/10.1016/j.desal.2014.12.036>.

Theydiffer, 2016. Difference Between Passive And Active Solar Energy. [online] 2 August. Available at: <<https://theydiffer.com/difference-between-passive-and-active-solar-energy/#:~:text=For%20these%20motors%20and%20electronic,materials%20used%20in%20the%20system>> [Accessed 09 September 2022].

Tofani, K. and Tiari, S., 2021. Nano-Enhanced Phase Change Materials in Latent Heat Thermal Energy Storage Systems: A Review. *Energies*, [e-journal] 14(13), p.3821. <https://doi.org/10.3390/en14133821>.

T.Suresh, A.Syed Abuthahir, A.Tamilazhagan, T.R.Sathishkumar, and S.Jegadeeswaran, 2011. A Review on Modified Solar Stills with Thermal Energy Storage and Fins. *International Research Journal of Engineering and Technology*, [e-journal] 4(10), pp.1216- 1236.

United Nations Water, 2022. *Water Scarcity*. [Online] Switzerland: United Nations Water. Available at: <<https://www.unwater.org/water-facts/scarcity/>> [Accessed 23 April 2022].

Velayutham, T., 2019. The importance of water in our daily lives. [Blog] *India Home Healthcare*, Available at: <<https://www.indiahomehealthcare.com/blogpost/the-importance-of-water-in-our-daily-lives/>> [Accessed 23 April 2022].

Vinay Kumar, B., 2015. Preparation And Characterization Of Paraffin/Palmitic Acid Eutectic Mixture In Thermal Energy Storage Applications. *International Journal of Mechanical Engineering and Robotics Research*, [e-journal] 4(1), pp123-127. <https://doi.org/10.18178/ijmerr>.

Wisut C., Derek F., Chun C.F., and Gerrard P., 2020. Solar Thermal Energy Stills for Desalination: A Review of Designs, Operational Parameters and Material Advances . *Journal of Energy and Power Technology*, [e-journal]. 2(4), p. 48. <https://doi.org/10.21926/jept.2004018>.

World Vision, 2022. *Global water crisis: Facts, FAQs, and how to help*. [Online]. Australia: World Vision. Available at: <<https://www.worldvision.com.au/global-water-crisis-facts#>> [Accessed 23 April 2022].

Zhi Y.H., Rubina B., Chai H.K., 2022. Passive solar stills coupled with Fresnel lens and phase change material for sustainable solar desalination in the tropics. *Journal of Cleaner Production*, [e-journal] 334(2022). pp.130279, <https://doi.org/10.1016/j.jclepro.2021.130279>.

Zhou, D., Zhou, Y., Yuan, J. and Liu, Y., 2020. Palmitic Acid-Stearic Acid/Expanded Graphite as Form-Stable Composite Phase-Change Material for

Latent Heat Thermal Energy Storage. *Journal of Nanomaterials*, [e-journal] 2020, pp.1-9. <https://doi.org/10.1155/2020/1648080>.

APPENDICES

Appendix A: Figures

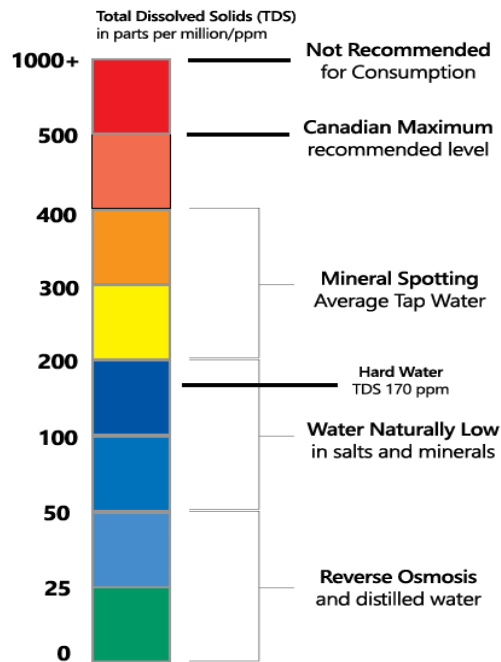


Figure A.1: TDS water chart (Jeff Wahl, 2021)

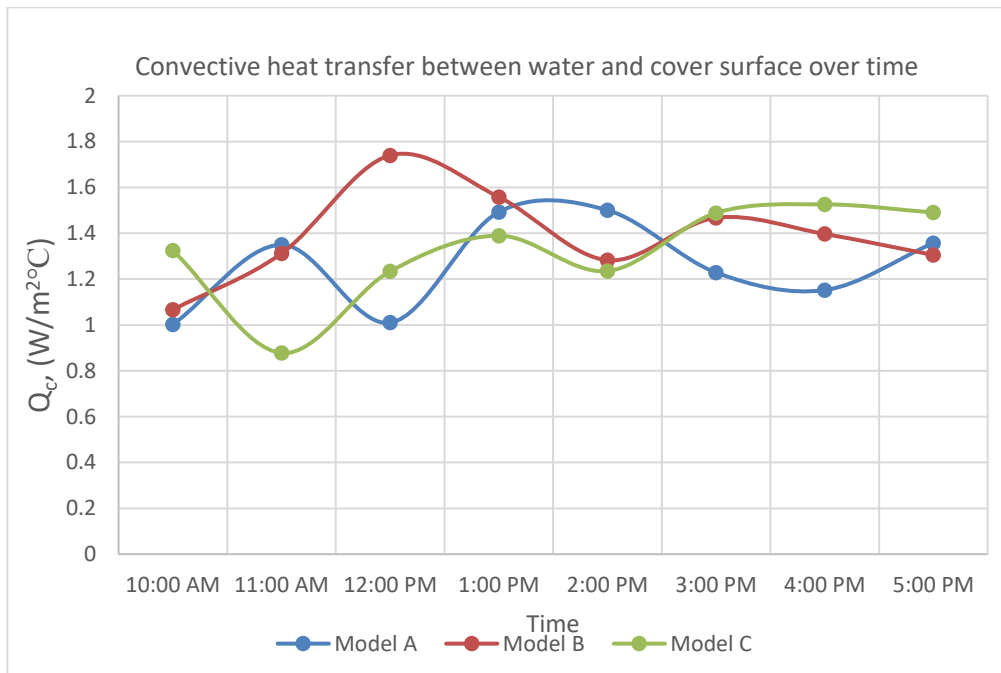


Figure A.2: Convective heat transfer of 3 model in 1st experiment (calculate based on experiment data).

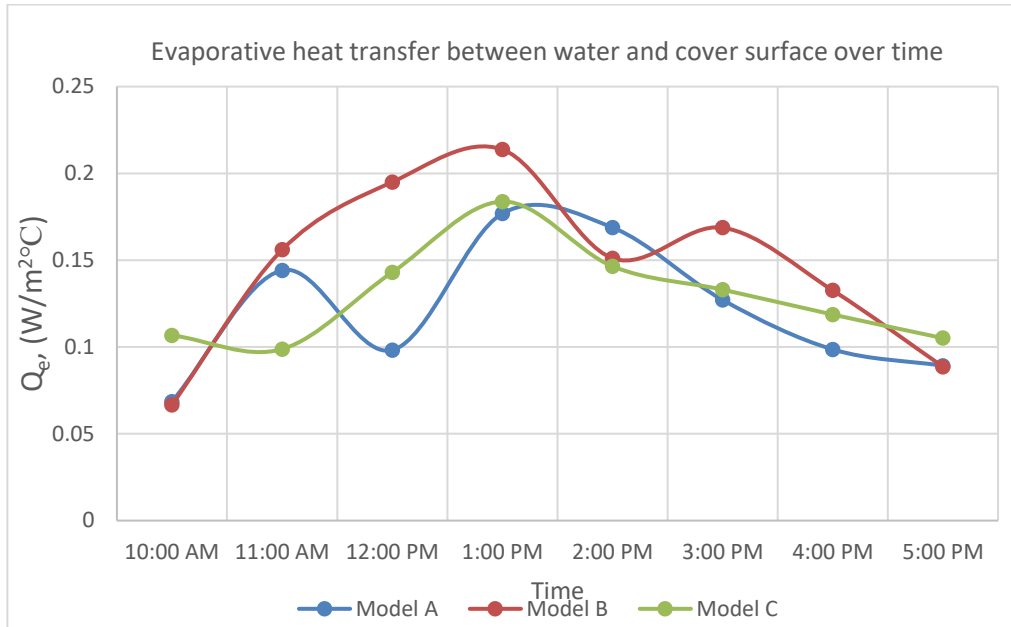


Figure A.3: Evaporative heat transfer of 3 model in 1st experiment (calculate based on experiment data).

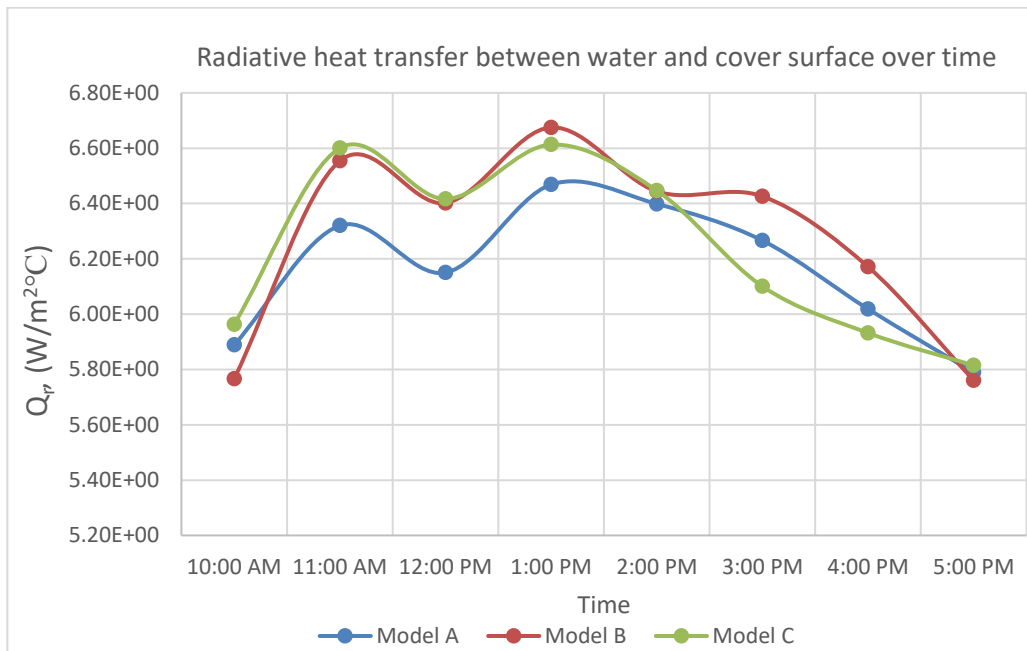


Figure A.4: Radiative heat transfer of 3 model in 1st experiment (calculate based on experiment data).

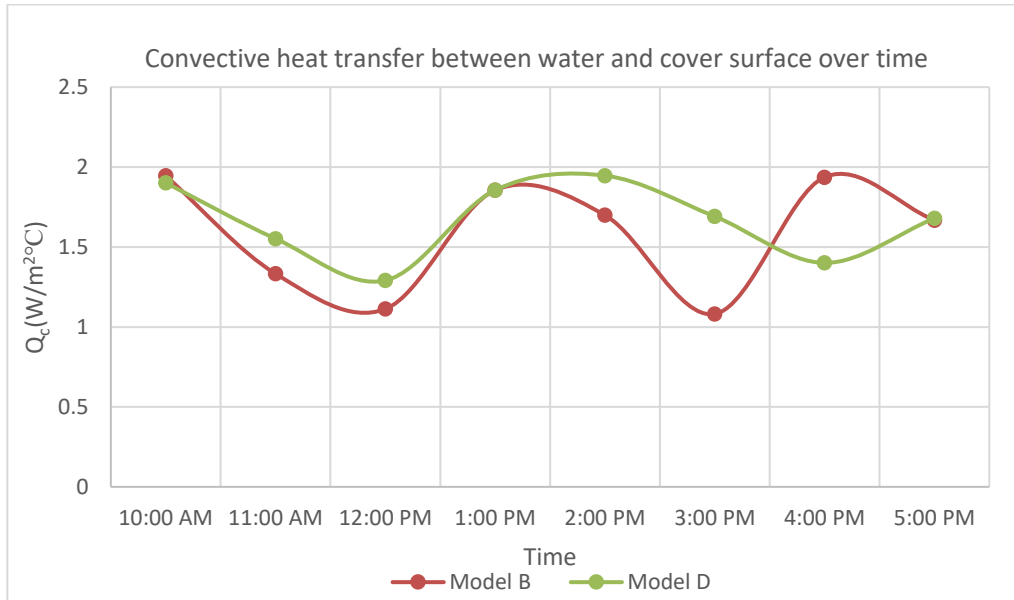


Figure A.5: Convective heat transfer of model B and D in 2nd experiment (calculate based on experiment data).

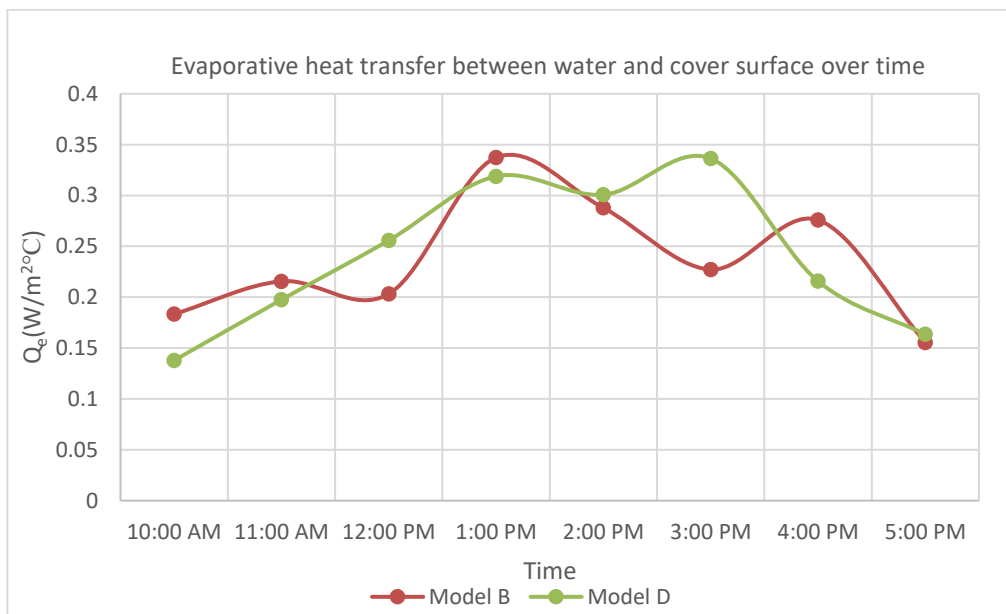


Figure A.6: Evaporative heat transfer of model B and D in 2nd experiment (calculate based on experiment data).

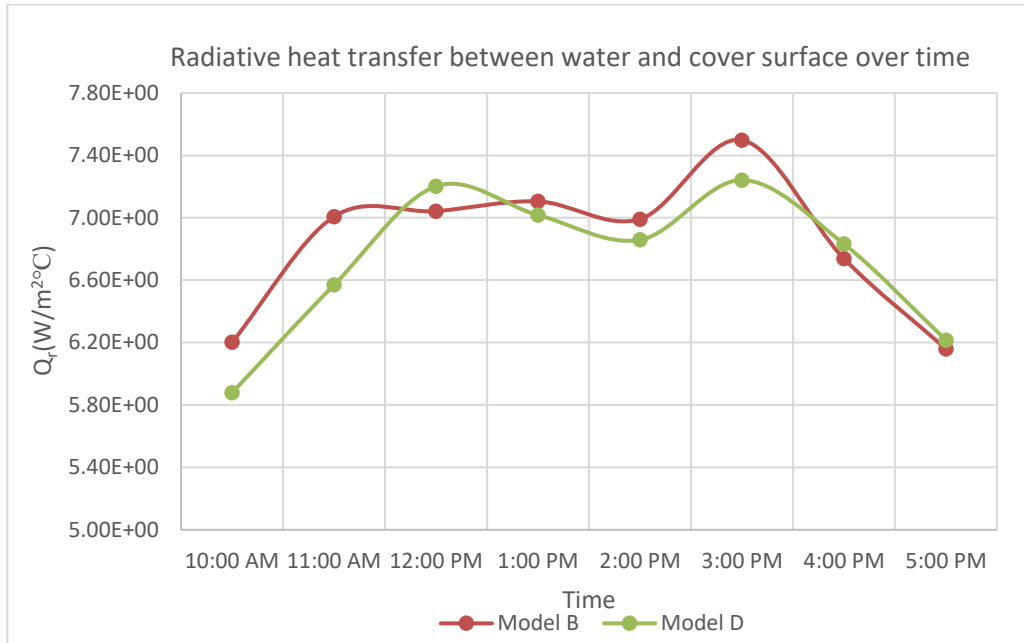


Figure A.7: Radiative heat transfer of model B and D in 2nd experiment (calculate based on experiment data).

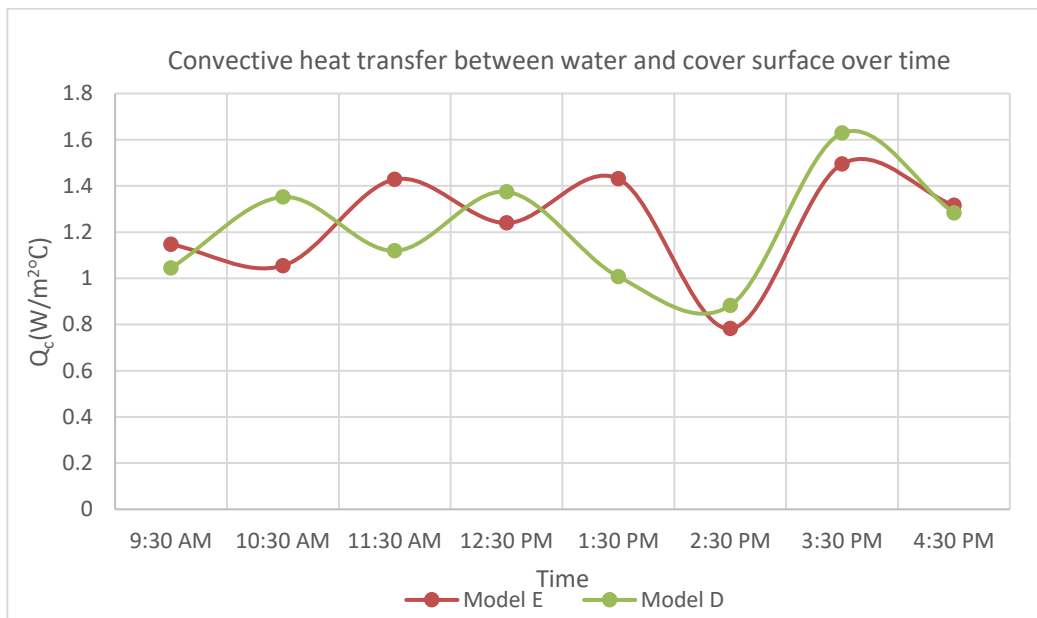


Figure A.8: Convective heat transfer of model E and D in 3rd experiment (calculate based on experiment data).

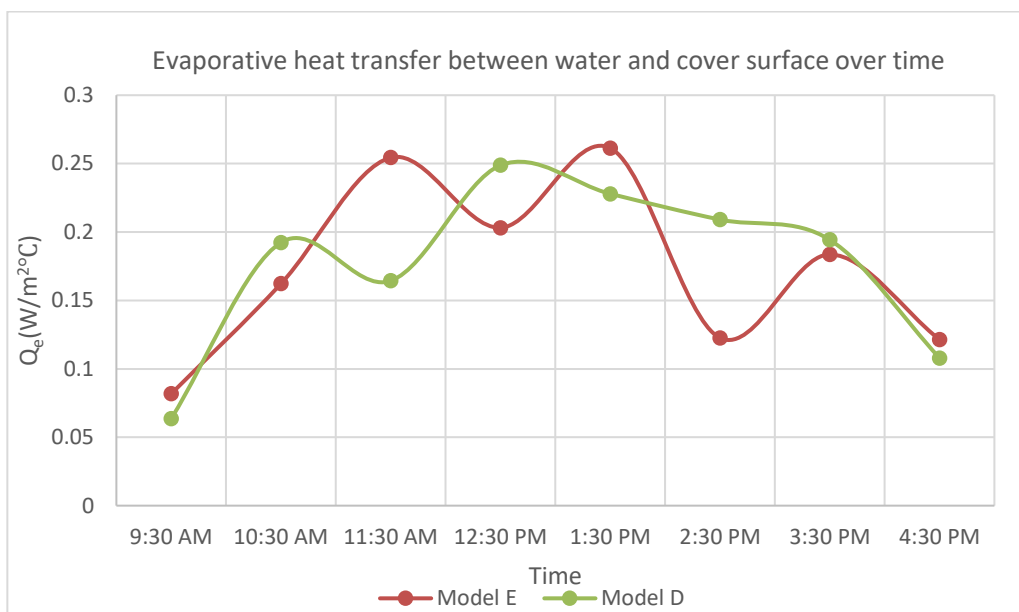


Figure A.9: Evaporative heat transfer of model E and D in 3rd experiment (calculate based on experiment data).

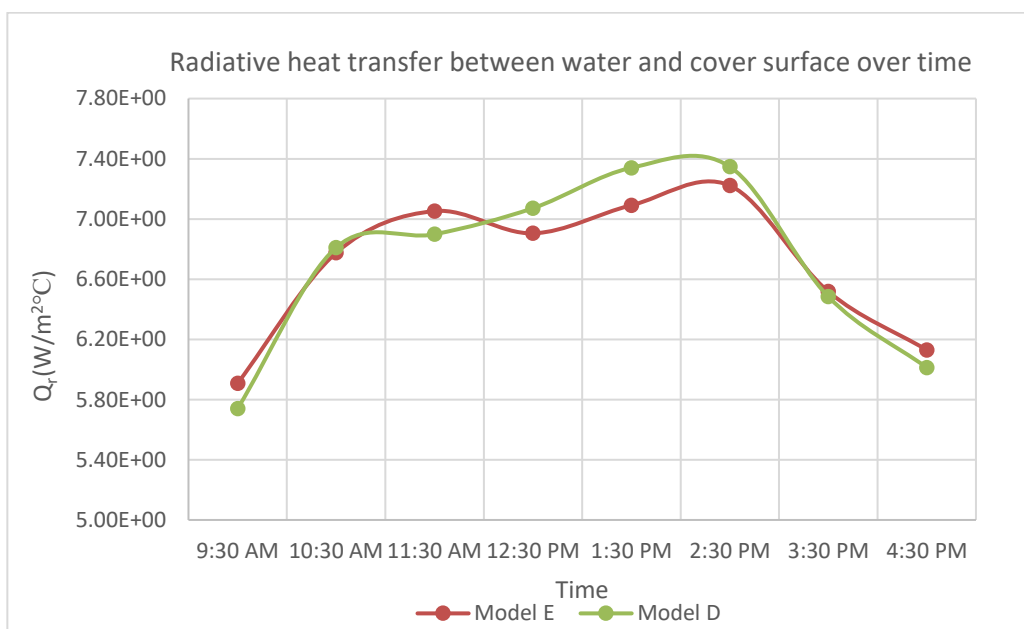


Figure A.10: Radiative heat transfer of model E and D in 3rd experiment (calculate based on experiment data).

Appendix B: Tables

Table B.1: Properties of Organic PCMs (Paraffin)

Fig 1 ID	Paraffin Name	Chemical Formula	CAS Number	Dominant Solid-Solid Temp (°C)	Solid-Solid Enthalpy (J/g)	Solid-Liquid Temp (°C)	Solid-Liquid Enthalpy (J/g)	Density (kg/m ³)	Cost (\$/kg)	Thermophysical property sources
P1	Tetradecane	C ₁₄ H ₃₀	629-59-4	-79	0.9	5.2 - 15.6	215 - 227	759	1 – 20	(Domalski & Hearing, 1996; Mondieig et al., 2004)
P2	Pentadecane	C ₁₅ H ₃₂	629-62-9	-3 – -2	41 - 43	9.6 - 10.0	161 – 163	765	1 – 45	(Domalski & Hearing, 1996; Mondieig et al., 2004)
P3	Hexadecane	C ₁₆ H ₃₄	544-76-3	–	–	17.6 - 18.2	228 – 236	770	1 – 20	(Domalski & Hearing, 1996; Mondieig et al., 2004)
P4	Heptadecane	C ₁₇ H ₃₆	629-78-7	11	45 - 46	21.6 - 22.0	164 – 167	775	1 – 15	(Domalski & Hearing, 1996; Mondieig et al., 2004)
P5	Octadecane	C ₁₈ H ₃₈	593-45-3	–	–	27.6 - 28.4	236 – 242	779	1 – 20	(Domalski & Hearing, 1996; Mondieig et al., 2004)
P6	Nonadecane	C ₁₉ H ₄₀	629-92-5	22 – 23	47 - 51	30.8 - 32.0	159 – 176	782	1 – 100	(Domalski & Hearing, 1996; Mondieig et al., 2004)
P7	Icosane	C ₂₀ H ₄₂	112-95-8	–	–	35.4 - 36.9	218 – 251	785	1 – 20	(Domalski & Hearing, 1996; Mondieig et al., 2004)
P8	Heneicosane	C ₂₁ H ₄₄	629-94-7	31 - 33	52 - 56	39.9 - 40.3	155 – 161	788	8 – 100	(Domalski & Hearing, 1996; Mondieig et al., 2004)
P9	Docosane	C ₂₂ H ₄₆	629-97-0	40 - 43	29 - 128	41.3 - 44.1	49 – 253	791	1 – 25	(Domalski & Hearing, 1996; Mondieig et al., 2004)
-	Tricosane	C ₂₃ H ₄₈	638-67-5	39 - 41	60 - 67	46.6 - 47.7	161 – 236	793	1 – 100	(Domalski & Hearing, 1996; Mondieig et al., 2004)
P11	Tetracosane	C ₂₄ H ₅₀	646-31-1	46 - 51	82 - 93	48.9 - 50.7	159 – 241	796	1 – 25	(Domalski & Hearing, 1996; Mondieig et al., 2004)
P12	Pentacosane	C ₂₅ H ₅₂	629-99-2	47 - 53	67 - 75	53.1 - 53.6	160 – 225	798	1 – 100	(Domalski & Hearing, 1996; Mondieig et al., 2004)
-	Hexacosane	C ₂₆ H ₅₄	630-01-3	50 - 53	83 - 95	56.0 - 56.5	160 – 174	800	15,620	(Domalski & Hearing, 1996; Mondieig et al., 2004)
-	Heptacosane	C ₂₇ H ₅₆	593-49-7	47 - 53	71 - 76	58.5 - 58.8	159 – 165	802	255,000	(Domalski & Hearing, 1996; Mondieig et al., 2004)
P15	Octacosane	C ₂₈ H ₅₈	630-02-4	56 - 58	85 - 90	60.3 - 61.6	160 – 169	803	2.10 – 100	(Domalski & Hearing, 1996; Mondieig et al., 2004)
-	Nonacosane	C ₂₉ H ₆₀	630-03-5	58 - 58	73 - 73	63.4	162	805	10 – 100	(Domalski & Hearing, 1996)
-	Triacotane	C ₃₀ H ₆₂	638-68-6	59 - 62	86 - 89	65.5 - 65.6	163	806	16,800	(Domalski & Hearing, 1996)
P18	Paraffin 46-50	–	–	20	–	43.0	228	765	0.99 – 1.76	(Ukrainczyk et al., 2010)
P19	Paraffin 52-54	–	–	20	–	53.0	220	774	0.72 – 1.50	(Ukrainczyk et al., 2010)
P20	Paraffin 58-62	–	–	27	–	60.0	206	782	0.45 – 0.90	(Ukrainczyk et al., 2010)
P21	Paraffin 62-70	–	–	25	–	62.0	201	799	0.45 – 1.10	(Ukrainczyk et al., 2010)

Table B.2: Properties of Organic PCMs (non-Paraffin)

Fig. 1 ID	Fatty Acid	Structural Chemical Formula	CAS Number	Melting Temperature (°C)	Melting Enthalpy (J/g)	Density (kg/m ³)	Cost (\$/kg)	Thermophysical property sources
AC1	Formic Acid Methanoic Acid	HCOOH	64-18-6	7.8 – 8.4	247	1200	0.36 - 0.68	(Veerakumar & Sreekumar, 2016)
AC2	Pelargonic Acid Nonanoic Acid*	CH ₃ (CH ₂) ₇ COOH	112-05-0	12.5	128	900	0.90 - 10.60	(Acree, 1991)
AC3	α -Oleic Acid	CH ₃ (CH ₂) ₇ CH=CH(CH ₂) ₇ COOH	112-80-1	13.3	76 – 140	895	0.80 - 3.50	(Acree, 1991; Cedeño et al., 2001; Sato et al., 1997)
AC4	β -Oleic Acid	CH ₃ (CH ₂) ₇ CH=CH(CH ₂) ₇ COOH	112-80-1	16.0 – 16.3	173 – 205	895	0.80 - 3.50	(Cedeño et al., 2001; Sato et al., 1997)
-	Caprylic Acid Octanoic acid	CH ₃ (CH ₂) ₆ COOH	124-07-2	16.3 – 16.7	135 – 148	910	3.50 - 120.00	(Acree, 1991; Domalski & Hearing, 1996)
AC6	Acetic Acid Ethanoic Acid	CH ₃ COOH	64-19-7	16 – 16.91	180 – 195	1270	0.40 - 1.20	(Julius, 1910; Parks & Kelley, 1925; Pickering, 1895)
-	Undecylic Acid Undecanoic Acid*	CH ₃ (CH ₂) ₉ COOH	112-37-8	28.6	139	890	1 - 5	(Domalski & Hearing, 1996)
AC8	Capric Acid Decanoic Acid	CH ₃ (CH ₂) ₈ COOH	334-48-5	31 – 32.13	152.7 – 162.7	885	1 - 100	(Hobi Bordón Sosa et al., 2019; Saeed et al., 2016; A. Sharma et al., 2005)
-	Petroselinic Acid ω -6-Octadecenoic Acid*	CH ₃ (CH ₂) ₁₀ CH=CH(CH ₂) ₄ COOH	593-39-5	30.5	168	900	10 - 100	(Sato et al., 1997)
-	Tridecylic Acid Tridecanoic Acid*	CH ₃ (CH ₂) ₁₁ COOH	638-53-9	41.5	157	983	20 - 150	(Domalski & Hearing, 1996)
AC11	Lauric Acid Dodecanoic Acid	CH ₃ (CH ₂) ₁₀ COOH	143-07-7	44 – 44.92	177.4 – 181.5	903	2.00 - 200	(Hobi Bordón Sosa et al., 2019; Saeed et al., 2016; A. Sharma et al., 2005)
AC12	Elaidic Acid*	CH ₃ (CH ₂) ₇ CH=CH(CH ₂) ₇ COOH	112-79-8	43.9 – 44.5	190 – 218	873	1 - 50	(Wilson et al., 2015)
-	Pentadecanoic Acid*	CH ₃ (CH ₂) ₁₃ COOH	1002-84-2	52.5	188	842	50 - 150	(Wilson et al., 2015)
AC14	Myristic Acid Tetradecanoic Acid	CH ₃ (CH ₂) ₁₂ COOH	544-63-8	54.2 – 58	191 – 198	962	1 - 120	(Hobi Bordón Sosa et al., 2019; Saeed et al., 2016; A. Sharma et al., 2005)
-	Margaric Acid Heptadecanoic Acid*	CH ₃ (CH ₂) ₁₅ COOH	506-12-7	61.2 – 61.3	217	853	2500 - 7500	(Wilson et al., 2015)
AC16	Palmitic Acid Hexadecanoic Acid	CH ₃ (CH ₂) ₁₄ COOH	57-10-3	62.5 – 64	163 – 212	886	2 - 150	(Hobi Bordón Sosa et al., 2019; Saeed et al., 2016; A. Sharma et al., 2005)

* Single primary measurement or no primary measurement found

Table B.3: Specification of solar stills



	Model A	Model B	Model C
Dimension of wood frame, mm	L x W:185x118 H:108(back); 68(front) Thickness: 6	L x W:203x130 H:116(back); 76(front) Thickness: 1.1; 6 (bottom)	L x W:190x123 H:116(back); 76(front) Thickness: 6
Dimension of water basin, mm			
Dimension of PCM/NePCM basin, mm	-		
Gap distance, mm	66	66	66
Tilt angle	19	19	19
Cover thickness and material	3mm Acrylic	3mm Acrylic	3mm Acrylic
Insulation	XPE	XPE	XPE

Table B.4: PCM specifications

	Paraffin wax	Soft paraffin
Specific heat capacity, kJ/kg K	2.14 – 2.9	-
Latent heat, kJ/kg	190	-
Melting point, °C	47 - 60 (Begin liquify at 40)	37 - 70
Thermal conductivity, W/m°C	0.21- 0.12	- (very low)
Density, g/cm ³	0.9	0.9
Volume of expansion	~15%	-
Physical state at room temperature	Solid	Semiliquid

Table B.5: Aluminium scarp and alumina nanopowder specifications

	Aluminium scarp	Alumina nanopowder
Thermal conductivity	202.4	40
Specific heat capacity, J/kg K	900	880
Particle density	-	1.5
Density g/cm ³	-	3.9
Size	1.5cm x 0.4cm x 0.1cm	30nm
Purity	-	>99.0%
Crystal structure	Aluminium plate sheet in workshop, cut into smaller pieces	α

Table B.6: Raw material cost for one model

Material	Cost, RM
Insulation (1pcs)	5.10
Wood frame	16.00
Acrylic cover (1pcs)	9.00
Aluminium tray – water basin (1pcs)	1.90
Aluminium tray – PCM basin (1pcs)	1.70
PCM – paraffin wax (50g)	2.50
Alumina nanoparticle (0.5g)	0.30
Miscellaneous (wood glue, tape, and others)	20.00
Total	56.50

Table B.7: Payback period of solar still without PCM, with pure paraffin wax, with NepCM (Al scrap and Alumina nano powder)

Material	Principal Cost, RM	Selling price, RM/250ml	Water Yield, g	Payback period, days
Without PCM	51.20	2.62	3.00	158
Pure paraffin wax	56.20		5.00	149
Al scrap + Paraffin wax	56.20		6.00	145
Alumina nano powder + Paraffin wax	56.50		7.00	142